[redacted]

~~SECRET~~ UNCLASSIFIED

Copy 4
RM E58D03b

NACA RM E58D03b

~~Copy 2~~

NACA

RESEARCH MEMORANDUM

THE EFFECT OF COMPRESSOR-INLET WATER INJECTION ON ENGINE AND AFTERBURNER PERFORMANCE

By Joseph N. Sivo, John P. Wanhainen, and William L. Jones

Lewis Flight Propulsion Laboratory
Cleveland, Ohio

CLASSIFICATION CHANGED

To UNCLASSIFIED

By authority of CSTAR Date 3-31-71
V-9 No. 1
I.N. 58-772 8/9/71

~~CLASSIFICATION CHANGED~~

~~CONFIDENTIAL~~

~~By authority of ______ Date ______~~

JUL 23 1958

CLASSIFIED DOCUMENT

NATIONAL ADVISORY COMMITTEE FOR AERONAUTICS

WASHINGTON

July 22, 1958

UNCLASSIFIED

~~SECRET~~

[redacted]

NACA RM E58D06 *U.B.* [redacted]

NATIONAL ADVISORY COMMITTEE FOR AERONAUTICS

RESEARCH MEMORANDUM

THE EFFECT OF COMPRESSOR-INLET WATER INJECTION ON ENGINE AND AFTERBURNER PERFORMANCE*

By Joseph N. Sivo, John P. Wanhainen, and
William L. Jones

SUMMARY

A turbojet engine incorporating a conventional-type afterburner was operated over a range of afterburner pressure levels from 1000 to 2000 pounds per square foot absolute and a range of engine-inlet water-air ratios from 0 to 0.08. At each pressure level and water-air ratio, the afterburner fuel flow was varied from lean blowout to maximum burner-outlet temperature.

On the basis of the experimental data obtained, it is apparent that substantial thrust gains will result from the injection of water ahead of the engine inlet at supersonic flight Mach numbers. However, as might be expected, the presence of the water vapor had an adverse effect on afterburner combustion efficiency and lean blowout limits. There was little if any effect of water injection on the afterburner efficiency above a 0.8 equivalence ratio at all pressure levels investigated. However, as the equivalence ratio was decreased below 0.8, efficiency decreased markedly as water-air ratio was increased. The stability of the afterburner was adversely affected by water injection with the equivalence ratio for lean blowout increasing with increasing water-air ratio. Decreasing the afterburner pressure level magnified the stability problem with water injection thus narrowing the operable range of the afterburner. For the range of pressure levels studied, the engine internal performance was reduced slightly in accordance with the change in gas properties due to the variation of water-air ratio covered in this investigation.

INTRODUCTION

The aircraft industry and the military services are very interested in the use of precompressor evaporative cooling using water injection to boost the performance of current interceptor aircraft. Analyses using this means of thrust augmentation have been made for aircraft at least of the 2-century series which show substantial increases in both flight Mach number and maximum altitude capability. These aircraft performance gains would not, for certain applications, result in a decrease in range or

*Title, ~~Secret~~ *Unclassified*

combat time, in view of the increase in rate of climb and cruise, or combat altitude. Precompressor cooling would also alleviate the engine temperature problems associated with Mach number increases. Most current turbojet engines encounter a temperature limitation in the compressor at ram temperatures corresponding to speeds in the neighborhood of Mach 2.0.

The full potential of water injection for providing superperformance can be achieved if major detrimental effects on afterburner and engine performance do not occur as a result of the presence of the water. The first, and perhaps the foremost problem area, would deal with the possible deleterious effects of water injection on the afterburner efficiency and operational limits. In this category possible detrimental effects on the engine itself are to be considered. Previous work in this area reported in references 1 and 2 has indicated that serious combustion problems may be present in the afterburner especially at high water-air ratios and low afterburner pressure levels. The second area deals with the water-injection system itself with its attendant problems of atomization and vaporization of the injected water, using hardware suitable for flight application. Some aspects of these problems are covered in reference 3. A bibliography of published reports relating to this field is also included in reference 3.

The investigation reported here determined the effect of various amounts of water vapor on afterburner and engine performance. To simplify the experiment, it was desired that the study of the effects be isolated from the problems of providing a water-injection system with a high evaporative effectiveness. Consequently, water vapor was provided by injecting steam into the engine-inlet airflow.

The engine was operated over a range of compressor-inlet total pressures from 1150 to 550 pounds per square foot absolute. The compressor-inlet temperature was held constant at 150° F as the water-air ratio was varied from 0 to 0.08. The afterburner operated over a range of inlet total pressures from 2000 to 1000 pounds per square foot absolute. This afterburner pressure range corresponds to operating a typical current turbojet engine at a Mach number of 2.0 over a range of altitudes from about 55,000 to 70,000 feet or at a Mach number of 3.0 over an altitude range from 81,000 to 96,000 feet with sufficient water injection to cool the compressor-inlet air to 242° F.

APPARATUS

Engine

A schematic diagram of the engine used in this investigation is shown in figure 1. The engine consisted of an axial-flow compressor with a moderate pressure ratio, an annular combustor, and a two-stage turbine. The maximum allowable compressor-inlet temperature for this engine is 150° F. A photograph of the engine installed in the altitude test chamber is shown in figure 2. The fuel used was JP-4, MIL-F-56-24A, having a low heating value of 18,700 Btu per pound.

Afterburner

A schematic diagram of the afterburner used is shown in figure 3. The burner incorporated a corrugated-louvered cooling liner which extended from a point 4 inches upstream of the flameholder to the inlet of the automatically-controlled variable-area iris-type exhaust nozzle. A solid liner extending from the corrugated-louvered cooling liner to a point just ahead of the spray bars was used to prevent circulation of fuel into the cooling-air passage. The flameholder was a conventional two-ring V-gutter type and is schematically shown in figure 4(a). The gutter width was $1\frac{5}{8}$ inches, and the blockage was approximately 33 percent of the full passage. The nominal afterburner-inlet velocity was 480 feet per second.

Afterburner Fuel System

The afterburner fuel-injection system consisted of 24 equally spaced radial spray bars. The bars were alternately axially staggered to ease installation problems, with the planes of injection being located 26 and 28 inches upstream of the flameholder. The spray bars, shown schematically in figure 4(b), consisted of eight 0.0225-inch-diameter holes on every bar with four located on each side to provide uniform fuel-air-ratio distribution. The fuel was injected normal to the gas stream. The fuel system conforms to the design criteria presented in reference 4.

Steam-Injection System

Steam was metered into the engine-inlet airflow at a point approximately 100 feet upstream of the engine inlet through a single fixed conical nozzle operating at or above the critical pressure ratio. The quality of the steam was determined with a throttling calorimeter.

Instrumentation

Location of the major instrumentation stations throughout the engine is shown in figure 1. A water-cooled total-pressure rake was installed at the exhaust-nozzle inlet. Both the engine and afterburner fuel flows were measured with vane-type remote-reading flowmeters. Total jet thrust was measured with a null-type thrust cell.

Installation

The engine was installed in an altitude test chamber that consisted of a tank 10 feet in diameter and 60 feet long divided into two compartments by a bulkhead. Ram pressure and temperature conditions are maintained in the front compartment; the engine was installed in the rear compartment where the altitude static pressure is maintained, and the engine-inlet duct extended through a labyrinth seal in the bulkhead to provide air at ram pressure and temperature to the engine. A bellmouth cowl and venturi were attached to the engine inlet to provide a means 4810 for measuring engine mass flow. The engine was mounted on a thrust-measuring platform in the rear compartment.

PROCEDURE

The engine was operated at rated engine speed with a constant turbine discharge temperature of 1200° F. The compressor-inlet temperature was maintained constant at 150° F. Three pressure levels at the compressor inlet were set to provide afterburner-inlet total-pressure levels of 2000, 1500, and 1000 pounds per square foot absolute. At a given pressure level and at constant compressor-inlet temperature, the compressor-inlet water-air ratio was varied from 0 to 0.08 by the steam injection. At each pressure level and compressor-inlet water-air ratio, the afterburner fuel-air ratio was varied from lean blowout to maximum burner-outlet temperature. The exhaust pressure was maintained at a value sufficient to insure critical flow through the exhaust nozzle.

RESULTS AND DISCUSSION

Although the primary objective of the investigation reported herein was to determine the effects of engine-inlet water injection on afterburner performance, engine performance data were also obtained during afterburner operation. The engine performance results are, therefore, included to give some insight into the effects of water injection on the engine for water completely evaporated before entering the compressor. These results indicate only the effects of water vapor on engine performance characteristics and, therefore, exclude any additional effects attributable to water droplets entrained in the inlet air.

Effects of Water Vapor on Engine Performance

Over-all engine performance. - The effect of water injection on over-all engine performance is shown in figure 5. The performance results are shown as a percent of the performance with no water injection for an inlet pressure of 1150 pounds per square foot absolute. A Mach number scale is indicated on the abscissa of figure 5 which corresponds to the water-air-ratio scale for air cooled to 150° F with 100-percent evaporative effectiveness. The dashed curves of figure 5 show the decreases in performance for the engine used that would result if the compressor-inlet temperature were allowed to rise above 150° F in accordance with increasing flight Mach number.

At constant mechanical speed and constant compressor-inlet temperature, increasing the water-air ratio decreased the corrected speed as shown in figure 5(a). At moderate water-air ratios, the corrected-speed decrease is approximately proportional to the square root of the increase in the gas constant of the incoming water-air mixture. This decrease is only a small fraction of the decrease indicated by the dashed curve that would result without water injection. The engine total-pressure ratio (fig. 5(b)) decreases slightly with increasing water-air ratio. This decrease, although small, primarily results from the decrease in corrected engine speed. The engine corrected fuel flow (fig. 5(d)) remained very nearly constant as the water-air ratio was increased. The decreases in pressure ratio and corrected weight flow with decreasing inlet total pressure at a constant water-air ratio are attributed to Reynolds number effects. As might be expected, the presence of water vapor had a slightly adverse effect on internal engine performance as indicated by the drop in weight flow and engine pressure ratio. The magnitude of the effect agrees with the change in the gas properties of the fluid passing through the engine. No change in the volume capacity of the engine was noted. Although the total engine weight flow decreased with increasing water-air ratio, it was necessary to maintain at least constant fuel flow. This was required when the engine total-temperature rise was maintained constant to compensate for the rise in specific heat of the working fluid and the drop in combustion efficiency indicated in the next section.

Component performance. - The performance of the compressor, combustor, and turbine are shown in figures 6(a), (b), and (c), respectively. There was little if any effect of increasing the water-air ratio from 0 to 0.08 on compressor and turbine efficiencies; however, there was a slight decrease in combustion efficiency. Compressor and turbine total-pressure ratios changed because of changes in engine weight flow and fluid property changes. Combustor total-pressure loss was not effected by water-air-ratio changes.

Effects of Water Vapor on Afterburner Performance

Afterburner combustion efficiency. - Afterburner combustion efficiency as a function of afterburner equivalence ratio is shown in figure 7 for afterburner-inlet total-pressure levels of 2000, 1500, and 1000 pounds per square foot absolute. The afterburner equivalence ratio φ_{AB}

is defined as the ratio of the actual fuel-air ratio based on unburned air entering the afterburner to the stoichiometric fuel-air ratio. At the afterburner pressures of 2000 and 1500 pounds per square foot absolute (figs. 7(a) and (b), respectively), the maximum water-air ratio was limited by the available steam supply. However, at 1000 pounds per square foot absolute, stable afterburning could not be obtained at water-air ratios over 0.06 (fig. 7(c)). Above an equivalence ratio of 0.8, water injection had little if any effect on afterburner efficiency at all the pressure levels investigated. However, increasing the water-air ratio at equivalence ratios near lean blowout decreased afterburner efficiency substantially.

Afterburner stability. - The effects of water-air ratio on afterburner stability can be seen in figure 8 for the three pressure levels investigated. As the water-air ratio is increased, the afterburner equivalence ratio at lean blowout is increased. As the pressure level is decreased, the effects of water injection become more pronounced. At 1500 pounds per square foot absolute of afterburner-inlet pressure, satisfactory afterburner operation was obtained at a water-air ratio of 0.08 which indicated that operation with higher water-air ratios would be possible at high equivalence ratios. At 1000 pounds per square foot absolute, afterburner operation at a water-air ratio of 0.06 was very marginal requiring care to maintain stable afterburning. The marked decrease in efficiency in the region of lean blowout was probably caused, for the most part, by partial blowout of the afterburner and reduced rates of flame propagation as a result of water dilution of the incoming fuel charge.

The decrease in afterburner stability with increasing water-air ratios and decreasing pressure could present a serious problem since it may be necessary to throttle back the afterburner during cruise at Mach numbers requiring high rates of water injection. Furthermore, the substantial reductions in combustion efficiency at these reduced equivalence ratios and high water-air-ratio conditions must be considered when predicting aircraft performance with water injection.

Other afterburner variables. - The effect of water injection on afterburner-outlet total temperature is shown in figure 9. In most cases at a given afterburner equivalence ratio, the outlet temperature decreased 40° to 50° F for each percent in water-air ratio. This decrease in temperature occurs because the ratio of the afterburner fuel flow to the product of the specific heat of the working fluid and its flow rate decreases as the water-air ratio is increased. By neglecting small changes in the ratios of specific heats, the product of specific heat and mass flow remains approximately constant over the range of water-air ratios covered. It follows that with engine-inlet and turbine-outlet temperatures fixed, the afterburner fuel flow at constant equivalence ratio must decrease as the water-air ratio is increased.

The decrease in afterburner fuel flow that did occur is shown in figure 10 for a typical afterburner pressure level of 1500 pounds per square foot absolute. The variation in temperature with water-air ratio results primarily from a corresponding variation in afterburner fuel flow.

The afterburner total-pressure loss for the three pressure levels is shown in figure 11. At a constant afterburner equivalence ratio, a water-air-ratio increase caused a total-pressure-loss decrease. The pressure-loss decrease results from two factors. (1) A decrease in afterburner-inlet velocity, approximately 5 percent at 0.08 water-air ratio, accompanying the decrease in mass flow with increasing water-air ratio; this produces a friction-loss decrease. (2) The decrease in momentum pressure loss accompanying the decrease in afterburner temperature rise and decrease in afterburner-inlet velocity. Each factor accounts for about 50 percent of the pressure-loss decrease. The burner pressure-loss reduction will, of course, vary from one afterburner to another, depending on the inlet velocity, friction pressure loss, and combustion efficiency.

The modulation of exhaust-nozzle effective flow area required to operate at a given turbine-outlet temperature and afterburner equivalence ratio as water-air ratio varies is shown in figure 12. The required nozzle area at constant equivalence ratio decreases about 12 percent when the water-air ratio increases from 0 to 0.08. The decrease in area is due to a combined effect of lower exhaust gas temperature, higher exhaust-nozzle-inlet total pressure, and decreased weight flow. Each factor contributes about equally to area change.

Comparison of results with previous work. - A general comparison of the afterburner performance results reported herein was made with the performance results reported in references 1 and 2. In reference 2 where ammonia was used as the engine-inlet injectant, the effects of increasing the injectant flow on afterburner performance were similar to those reported herein. At low afterburner equivalence ratios the effect of the injectant was marked, and at high equivalence ratios the effect was negligible.

The results of the investigation reported in reference 1, where a mixture of water and alcohol was used as the injectant, indicate that the effects of liquid injection on afterburner performance were marked at high equivalence ratios and negligible at the low equivalence ratios. The equivalence ratio trend of reference 1 is opposite to the trend reported herein. Careful study of the data presented in reference 1 did not reveal any definite explanation for the difference. However, the afterburner fuel-air-ratio distribution was varied with liquid-injectant flow to eliminate afterburner screech. Although the afterburner performance (ref. 1) was checked at zero injectant flow and indicated no performance changes for each fuel-air distribution, it is possible that the magnitude of the effects of liquid injection could change as fuel-air-ratio distribution was altered. In the data reported herein a uniform fuel-air distribution was selected and maintained throughout the entire investigation, thereby eliminating any possible effects of changing fuel-air-ratio distribution

High Mach Number Performance With Water Injection

The proposed use of engine-inlet water injection will provide both temperature protection for the engine at high Mach numbers and a substantial amount of thrust augmentation. This section illustrates the performance of a typical Mach 2.0 turbojet utilizing water injection to extend its Mach number limit to 3.0.

For the purposes of the calculation, the engine is held at constant altitude above the tropopause, and the Mach number is increased from 0.7 to 3.0. The maximum allowable compressor-inlet temperature was assumed to be equal to the ram temperature at a Mach number of 2.0. At flight Mach numbers in excess of 2.0, water is injected at a rate sufficient to maintain this temperature assuming complete evaporation of the water before entering the compressor. The Aircraft Industries Association standard ram recovery was used for the engine-inlet recovery factor (fig. 13).

The computed water-air ratio required to cool the engine-inlet air as the Mach number increased is shown in figure 14. The net thrust and net thrust specific liquid consumption are shown in figure 15 as functions of the flight Mach number. The dashed line represents the performance of a current engine capable of operation up to a Mach number of 2.0. The performance of this engine has been extrapolated to a Mach number of 2.5 to illustrate performance trends. An altitude of 75,000 feet was selected for the performance calculations with water injection so that the afterburner pressure level could be acted on by the water-injection performance discussed herein.

The marked increase in the slope of the thrust curve at a Mach of 2.0 (fig. 15(a)) indicates that the presence of the water results in over-all engine-thrust augmentation. Figure 15(b) shows that the liquid consumption of the engine also increases very rapidly as the Mach number increases beyond Mach 2.0. The specific fuel consumption in the Mach number range from 2.0 to 3.0 during water injection is shown in figure 15(b) in order to indicate the relative consumption of water and fuel by the engine. This high liquid consumption with water injection would limit this type of augmentation to very specific applications, where gains in performance, increased acceleration, rate of climb, and cruise altitude sufficiently offset the increase in total liquid consumption.

SUMMARY OF RESULTS

From the results of this investigation, it is apparent that substantial thrust gains will result from the injection of water ahead of the engine inlet at supersonic flight Mach numbers. However, as might be expected, the presence of the water vapor had an adverse effect on afterburner combustion efficiency and lean blowout limits. There was little if any effect on the afterburner efficiency from the presence of water vapor above an afterburner equivalence ratio of 0.8 for afterburner-inlet pressures from 1000 to 2000 pounds per square foot absolute. However, as the equivalence ratio was reduced, the effects of water injection became increasingly pronounced resulting in reductions in afterburner efficiency of 10 percent or more near lean blowout. As might be expected, reductions in pressure level magnified the detrimental effects of water injection on efficiency at reduced equivalence ratios.

Afterburner stability was very noticeably affected by the introduction of water. This was the case at all pressure levels and was evidenced by increased equivalence ratios at lean blowout as the water-air ratio was increased. As the afterburner pressure level was reduced, the effects became more pronounced and resulted in a reduction in the operable range of the afterburner. At a pressure level of 1500 pounds per square foot absolute, operation to at least a 0.08 water-air ratio was possible above an equivalence ratio of 0.6, but at 1000 pounds per square foot absolute, marginal operation was encountered at a 0.06 water-air ratio. The seriousness of the adverse stability limit trend with water-air ratio is magnified by the fact that at high Mach number cruise conditions it will be necessary to throttle back the afterburner.

The presence of water vapor in the inlet air to the engine did have a slightly adverse effect on internal-engine performance. The magnitude of the effect was consistent with the change in the properties of the fluid passing through the engine.

Lewis Flight Propulsion Laboratory
National Advisory Committee for Aeronautics
Cleveland, Ohio, April 7, 1958

4810

CF-2

APPENDIX A

SYMBOLS

A	area, sq ft
C_{f1}	flow coefficient, inlet-air measuring station
C_p	specific heat, constant pressure 4810
C_V	velocity coefficient
F_j	measured jet thrust, lb
F_n	net thrust, lb
f	fuel-air ratio
g	acceleration of gravity, ft/sec^2
H_c	heating value of fuel, Btu/lb
h	enthalpy, Btu/lb
M_0	flight Mach number
m	mass flow, lb-sec/ft
P	total pressure, lb/sq ft
p	static pressure, lb/sq ft
R	gas constant, (ft)(lb)/(lb)($^{\circ}$R)
T	total temperature, $^{\circ}$R
V	velocity, ft/sec
w	weight flow, lb/sec
γ	ratio of specific heats
η	efficiency

φ equivalence ratio

Subscripts:

AB	afterburner
a	airflow
B	combustor
C	compressor
CL	compressor-seal leakage
cr	critical
e	engine
eff	effective
f	fuel
l	liquid
mx	mixture
T	turbine
Tf	turbine flange
t	total weight flow
w	water
0	free stream
1	airflow measuring station
2	compressor inlet
3	compressor outlet
4	turbine inlet
5	turbine outlet
9	exhaust-nozzle inlet
10	exhaust-nozzle discharge

APPENDIX B

METHODS OF CALCULATION

Airflow

Engine-inlet airflow was calculated from measurements at station 1 with the following equations:

4810

$$(1)\quad w_{mx,1} = C_{f1}A_1p_1\sqrt{\frac{g}{R_{mx}T_1}}\sqrt{\frac{2\gamma_{mx}}{\gamma_{mx}-1}\left(\frac{P}{p}\right)^{\frac{\gamma_{mx}-1}{\gamma_{mx}}}\left[\left(\frac{P}{p}\right)^{\frac{\gamma_{mx}-1}{\gamma_{mx}}}-1\right]}$$

$$(2)\quad \frac{w_w}{w_{a,1}} = \frac{w_w}{w_{mx,1} - w_{w,1}};\quad w_{a,1} = w_{mx,1} - w_w;$$

$$C_{p,mx} = \frac{w_w}{w_{mx}}C_{p,w} + \frac{w_a}{w_{mx}}C_{p,a};\quad R_{mx} = \frac{w_w}{w_{mx}}R_w + \frac{w_a}{w_{mx}}R_a;$$

$$\gamma_{mx} = \frac{C_{p,mx}}{C_{p,mx} - R_{mx}}$$

For the range of water-air ratios covered in this report, the variation of γ_{mx} at the engine inlet was considered negligible, and the γ for air was used in the flow equation. Steam flow was determined at the steam-injection station, and thus an iteration process using R_{mx} was used to calculate $w_{mx,1}$ and w_w/w_a. A flow coefficient C_{f1} of 0.994 was determined from the ratio of actual airflow to the one-dimensional calculation of airflow.

Weight Flows

$$w_{mx,1} = w_{a,1} + w_{w,1} = w_{mx,2}$$

$$w_{a,1} = w_{a,2}$$

$$w_{a,3} = w_{a,2} - w_{a,CL} - w_{a,Tf}$$

$$w_{a,4} = w_{a,3}$$

$$w_{a,5} = w_{a,4} + w_{a,Tf} = w_{a,9}$$

The compressor-seal leakage flow $w_{a,CL}$ and turbine-flange cooling flow were considered to be composed of air only to ease calculation procedure. This assumption has a negligible effect on engine and afterburner calculated performance.

4810

$$w_{mx,4} = w_{mx,2} - w_{a,CL} - w_{a,Tf} + w_{f,e}$$

$$w_{mx,5} = w_{mx,4} + w_{a,Tf}$$

$$w_{mx,9} = w_{mx,5} + w_{f,AB}$$

Compressor Efficiency

Compressor efficiency was calculated using the following equation:

$$\eta_C = \frac{\left. h_a \right]_{2\ \text{isentropic}}^{3} + \frac{w_w}{w_{a,2}} \left. h_w \right]_{2\ \text{isentropic}}^{3}}{\left. h_a \right]_{2\ \text{actual}}^{3} + \frac{w_w}{w_{a,2}} \left. h_w \right]_{2\ \text{actual}}^{3}}$$

Engine Combustion Efficiency

Engine combustion efficiency was calculated using the following equation:

$$\eta_e = \frac{\left. h_a \right]_{1}^{5} + f_{e,5}\lambda_5 + \frac{w_w}{w_{a,5}} \left. h_w \right]_{1}^{5} + \frac{w_{a,CL}}{w_{a,5}} \left. h_a \right]_{1}^{3}}{f_{e,5} H_c}$$

where λ_5 is as defined in reference 5.

Turbine Efficiency

Turbine efficiency was calculated using the following equation:

$$\eta_T = \frac{\left\{ (h_a + f_e \lambda) \Big]_5^4 + \frac{w_w}{w_{a,5}} h_w \Big]_5^4 \right\}_{actual}}{\left\{ (h_a + f_e \lambda) \Big]_5^4 + \frac{w_w}{w_a} h_w \Big]_5^4 \right\}_{isentropic}}$$

where λ is as defined in reference 5.

Afterburner-Outlet Total Temperature

Afterburner-outlet temperature was calculated using a measured value of jet thrust as follows:

$$T_9 = \frac{(F_j \text{ measured})^2}{\left(C_V \frac{w_{mx,9}}{g} \frac{V_{eff}}{\sqrt{gR_{mx,9}T_9}} \times \sqrt{gR_{mx,9}} \right)^2}$$

Where the value of $\frac{V_{eff}}{\sqrt{gRT_9}}$ is taken from reference 6, and the value of the velocity coefficient C_V was obtained from an exhaust-nozzle calibration.

Afterburner Combustion Efficiency

Afterburner combustion efficiency was calculated using the following equation:

$$\eta_{AB} = \frac{h_a \Big]_1^9 + (f_{e,5} + f_{AB,9})\lambda_9 + \frac{w_w}{w_{a,9}} h_w \Big]_1^9 - \left\{ h_a \Big]_1^5 + f_{e,5}\lambda_5 + \frac{w_w}{w_{a,5}} h_w \Big]_1^5 \right\}}{(1 - \eta_e) f_{e,5} H_c + f_{AB,9} H_c}$$

where $w_{a,5} = w_{a,9}$ and the effects of dissociation have been taken into account.

Exhaust-Nozzle Effective Area

The exhaust-nozzle effective flow area was calculated as follows:

$$A_{10,eff} = \left(\frac{P_9 A_{10}}{m_9 \sqrt{gR_{mx,9}T_9}}\right)_{cr} \times \frac{\sqrt{gR_{mx,9}T_9} \times \frac{w_{mx,9}}{g}}{P_9}$$

where the value of the total-pressure parameter $\left(\frac{PA}{m\sqrt{gRT}}\right)_{cr}$ for critical flow is taken from reference 6.

REFERENCES

1. Useller, James W., and Povolny, John H.: Experimental Investigation of Turbojet-Engine Thrust Augmentation by Combined Compressor Coolant Injection and Tail-Pipe Burning. NACA RM E51H16, 1951.

2. Useller, James W., Harp, James L., Jr., and Fenn, David B.: Turbojet-Engine Thrust Augmentation at Altitude by Combined Ammonia Injection into the Compressor Inlet and Afterburning. NACA RM E52L19, 1953.

3. Sohn, R. L., ed.: Theoretical and Experimental Studies of Pre-Compressor Evaporative Cooling for Application to the Turbojet Engine in High Altitude Supersonic Flight. TR 56-477, WADC, Aug. 31, 1956. (Contract No. AF33(616)-3069.)

4. Lundin, Bruce T., Gabriel, David S., and Fleming, William A.: Summary of NACA Research on Afterburners for Turbojet Engines. NACA RM E55L12, 1956.

5. Turner, L. Richard, and Bogart, Donald: Constant-Pressure Combustion Charts Including Effects of Diluent Addition. NACA Rep. 937, 1949. (Supersedes NACA TN's 1086 and 1655.)

6. Turner, L. Richard, Addie, Albert N., and Zimmerman, Richard H.: Charts for the Analysis of One-Dimensional Steady Compressible Flow. NACA TN 1419, 1948.

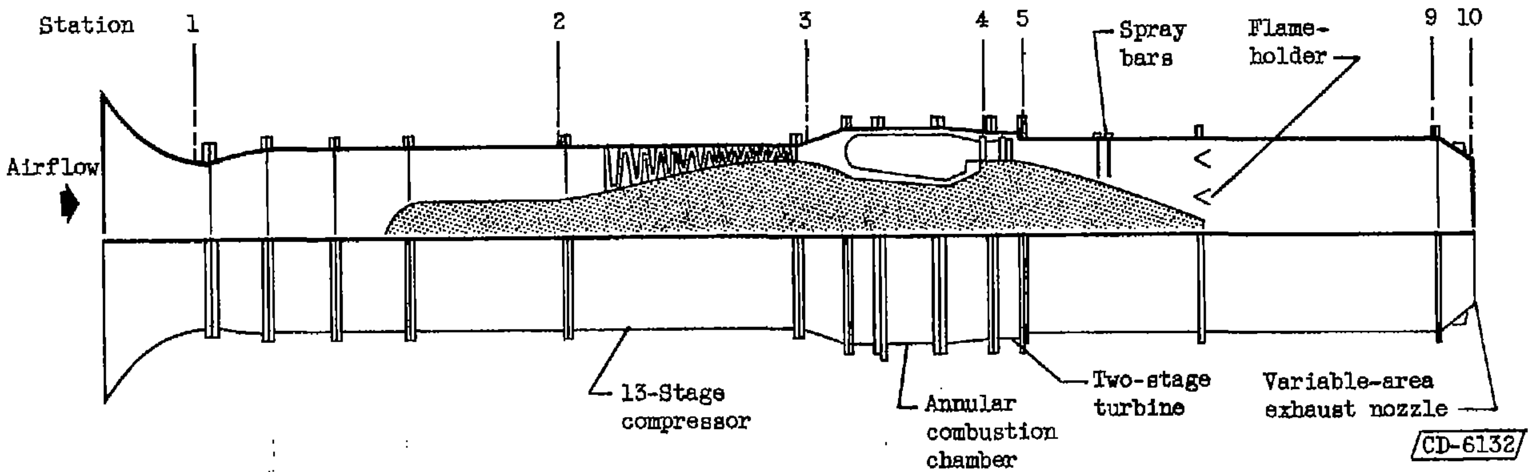

Figure 1. - Schematic diagram of the engine and afterburner showing location of instrumentation stations.

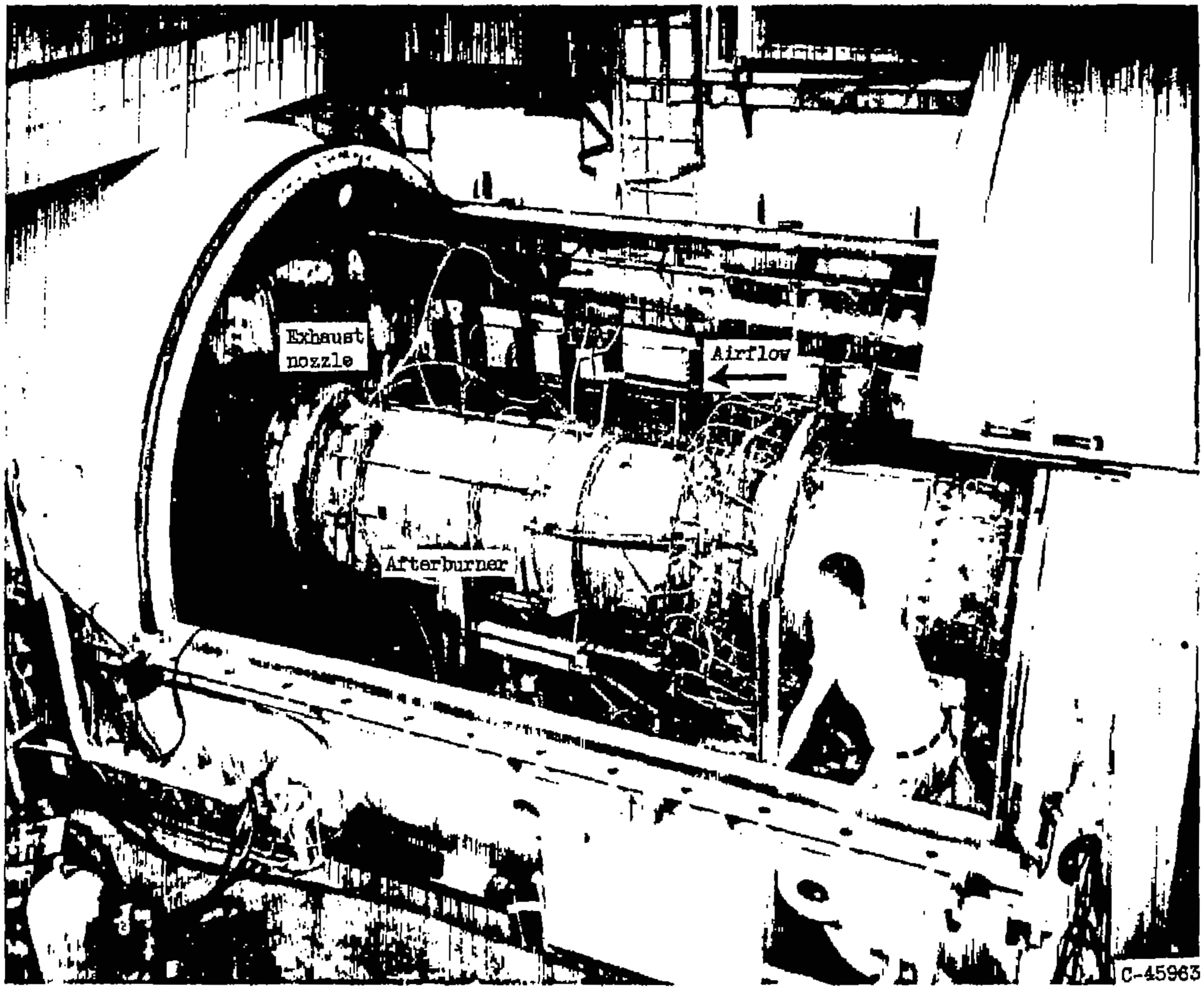

Figure 2. - Photograph showing engine and afterburner installed in the altitude test chamber.

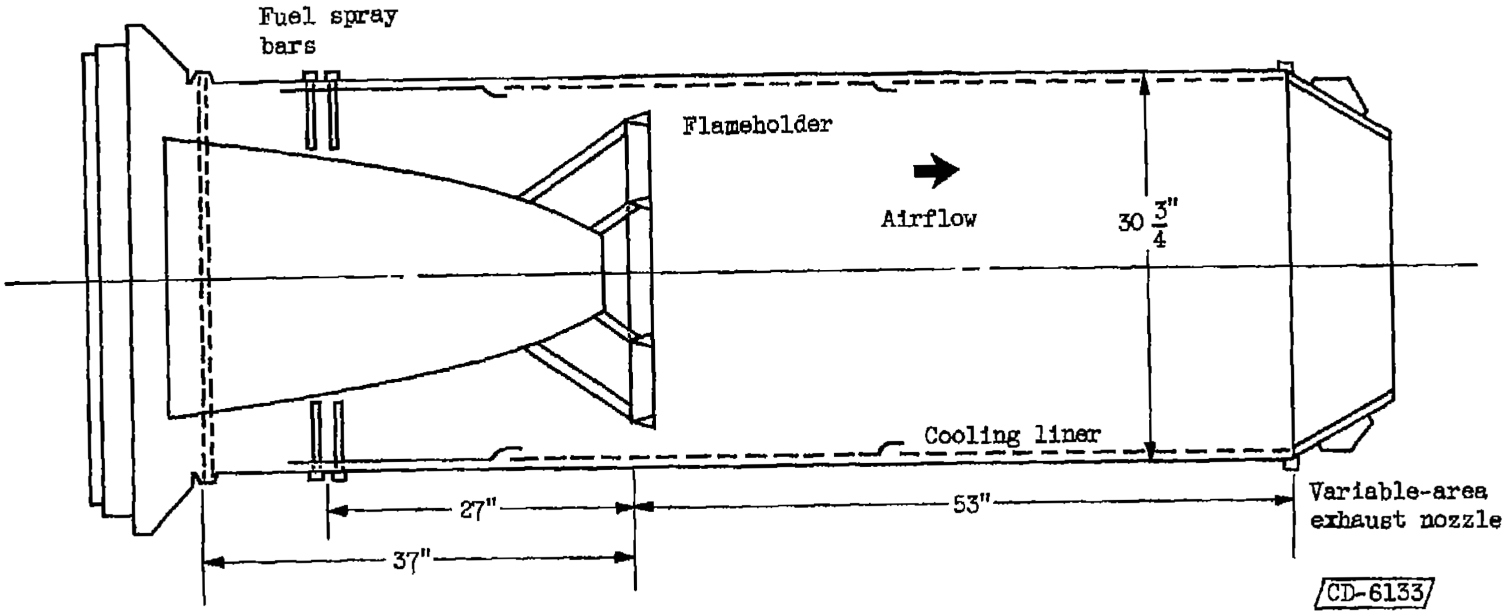

Figure 3. - Schematic diagram of the afterburner.

4810

CF-3 back

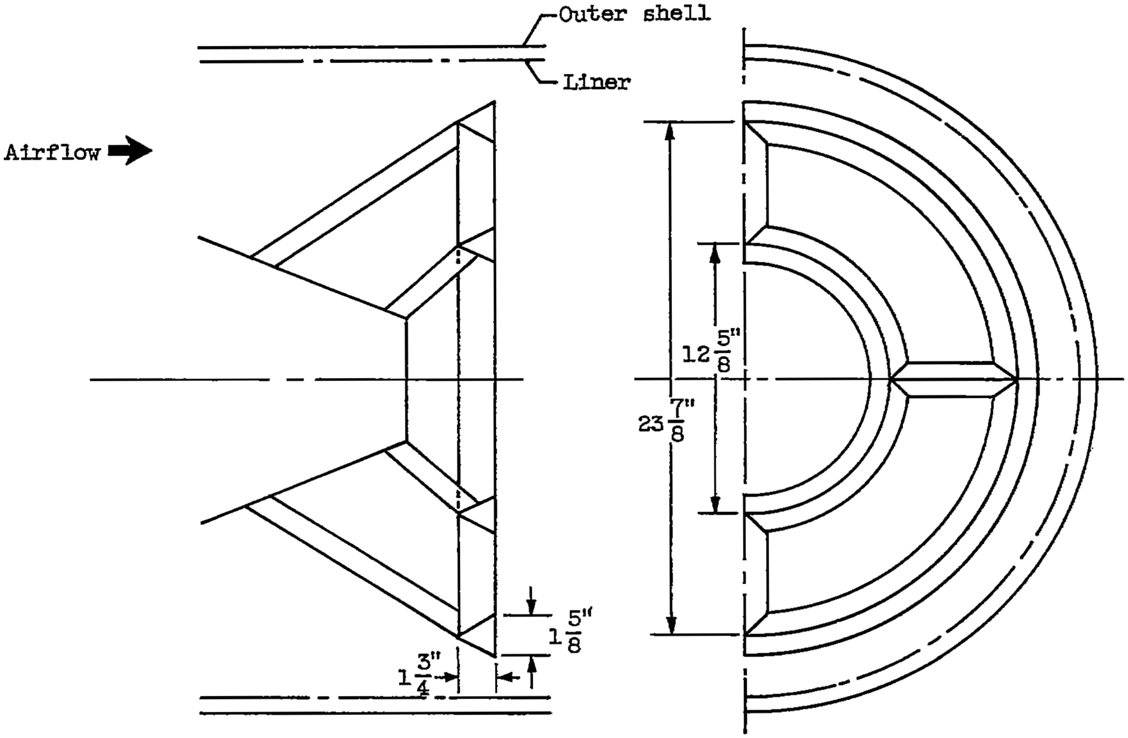

(a) Flameholder.

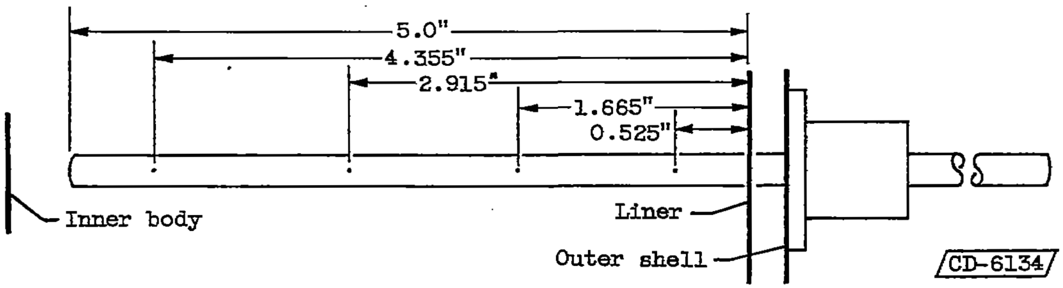

(b) Spray bar.

Figure 4. - Schematic sketches of flameholder and fuel spray bar.

[redacted]

4810

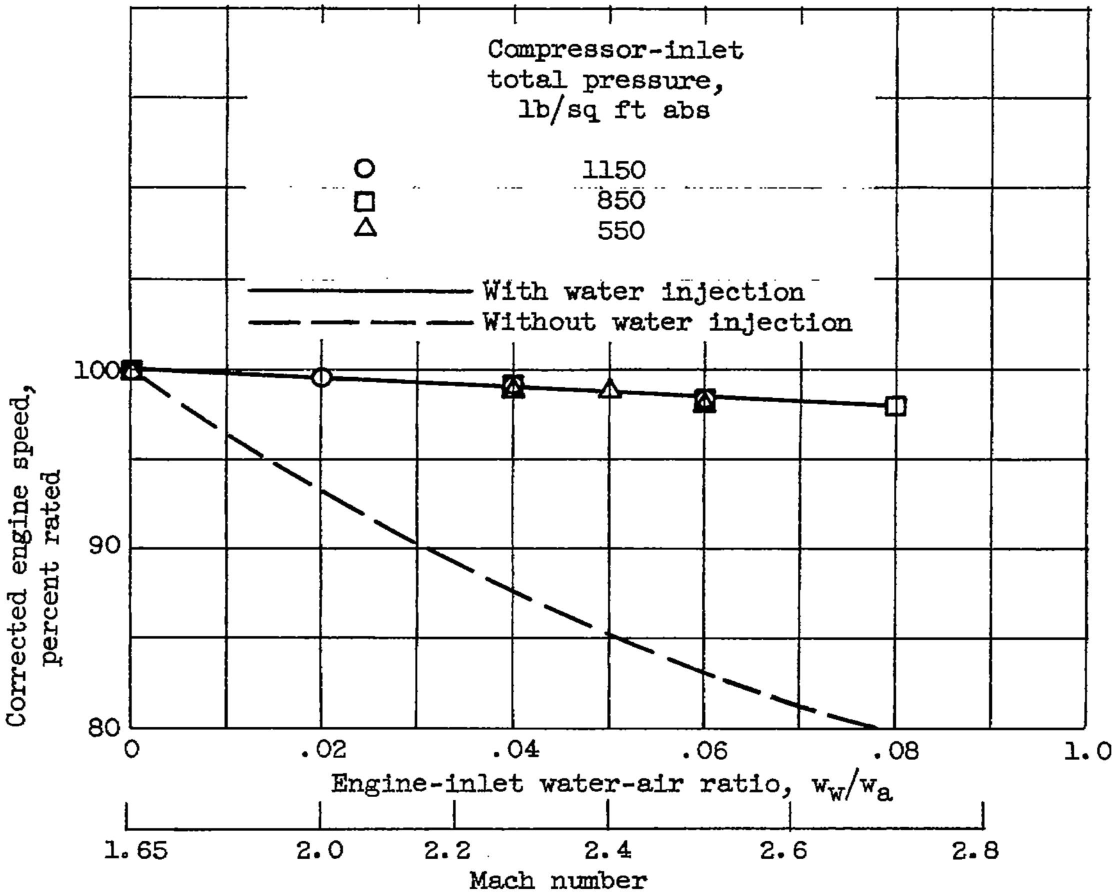

(a) Corrected engine speed.

Figure 5. - Effect of engine-inlet water injection on over-all engine performance.

4810

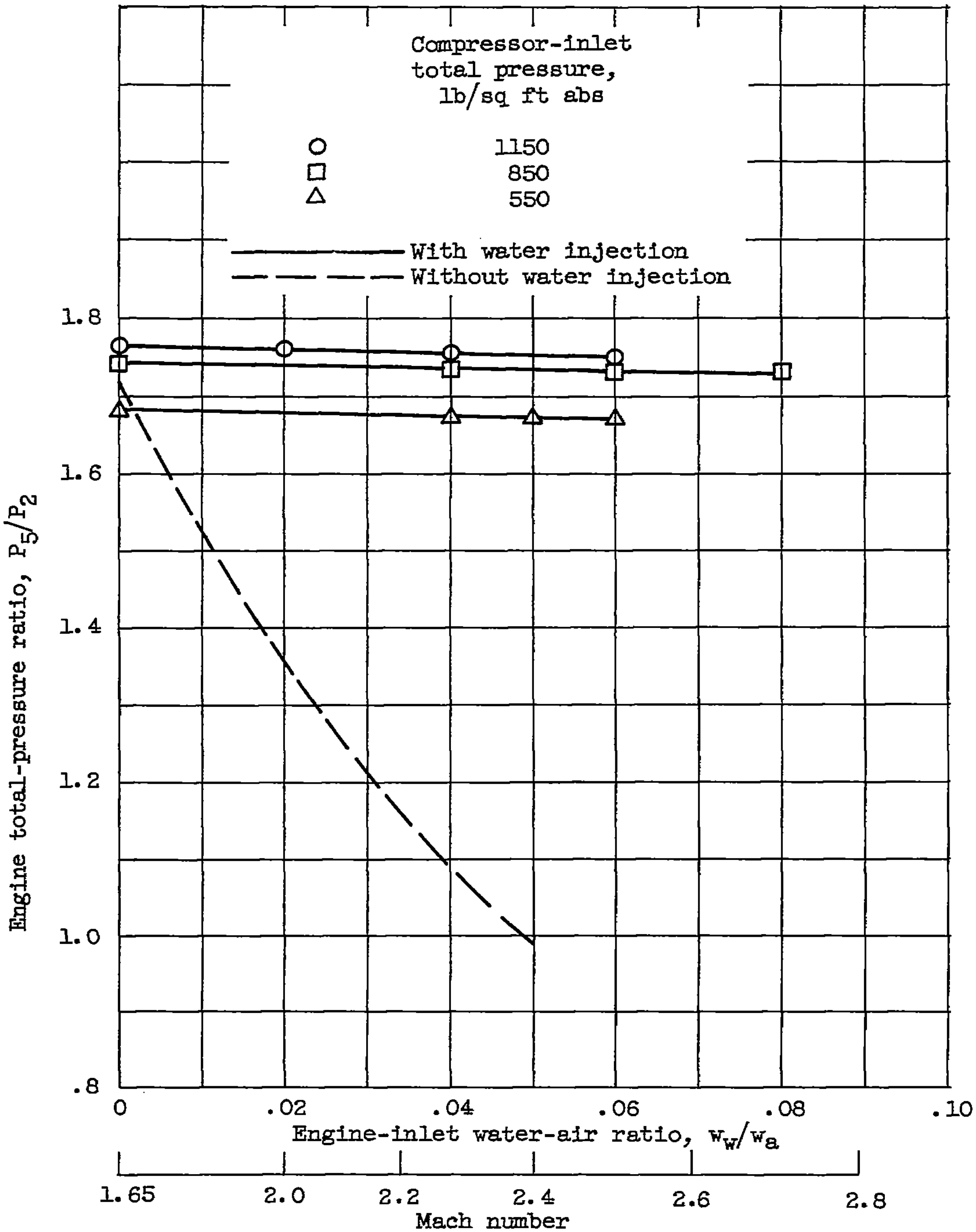

(b) Engine total-pressure ratio.

Figure 5. - Continued. Effect of engine-inlet water injection on over-all engine performance.

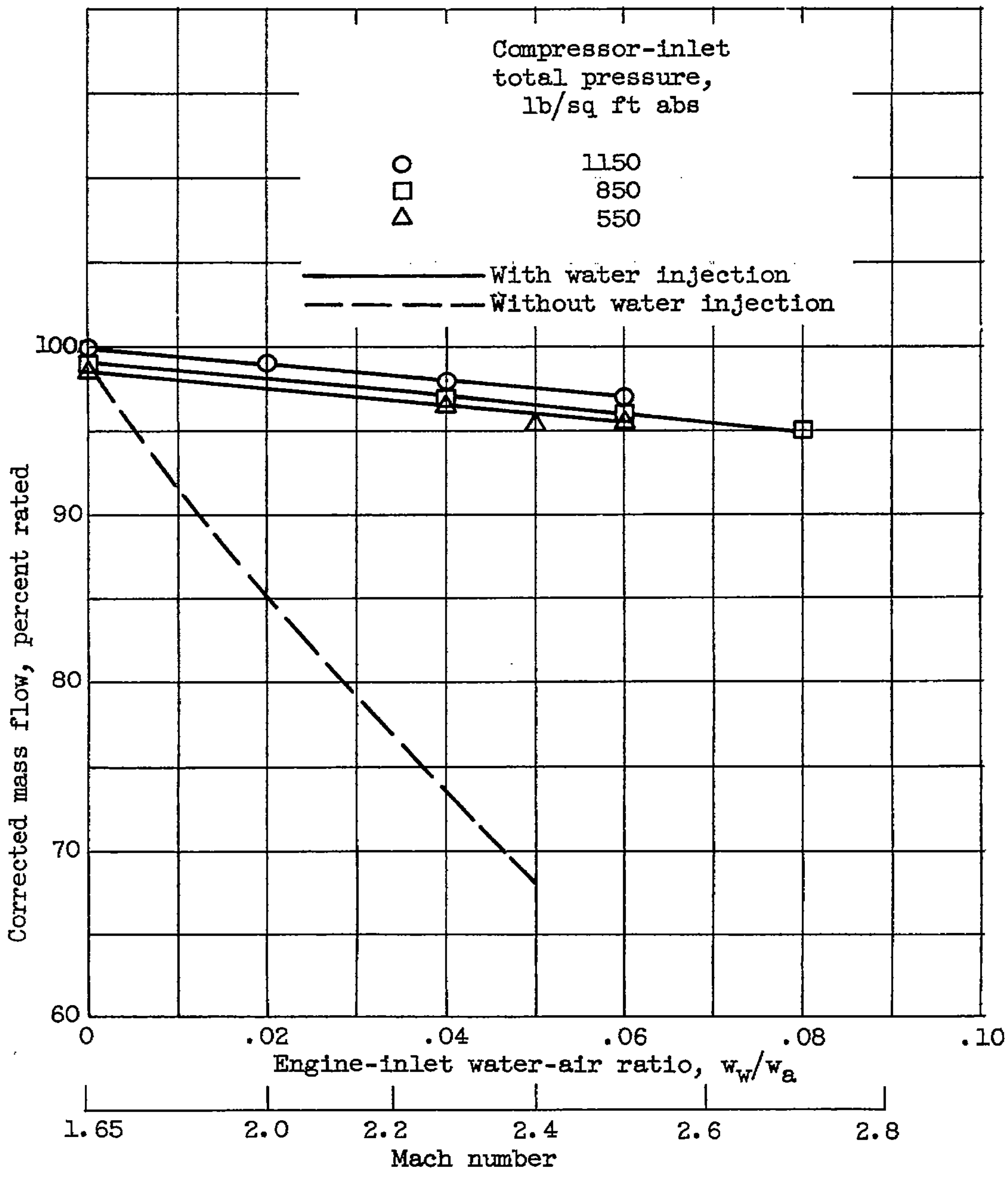

(c) Corrected engine-inlet mass flow.

Figure 5. - Continued. Effect of engine-inlet water injection on over-all engine performance.

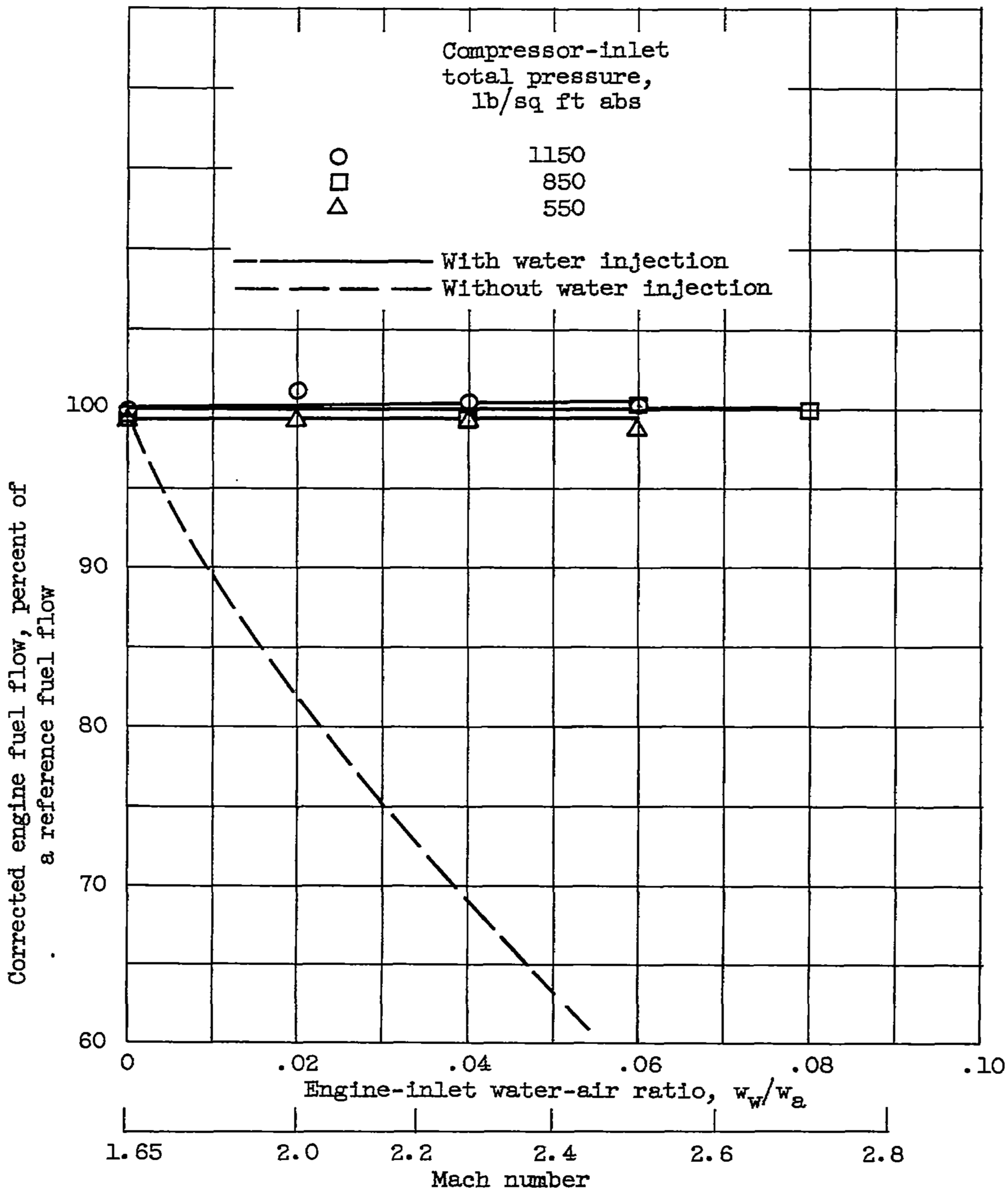

(d) Corrected engine fuel flow.

Figure 5. - Concluded. Effect of engine-inlet water injection on over-all engine performance.

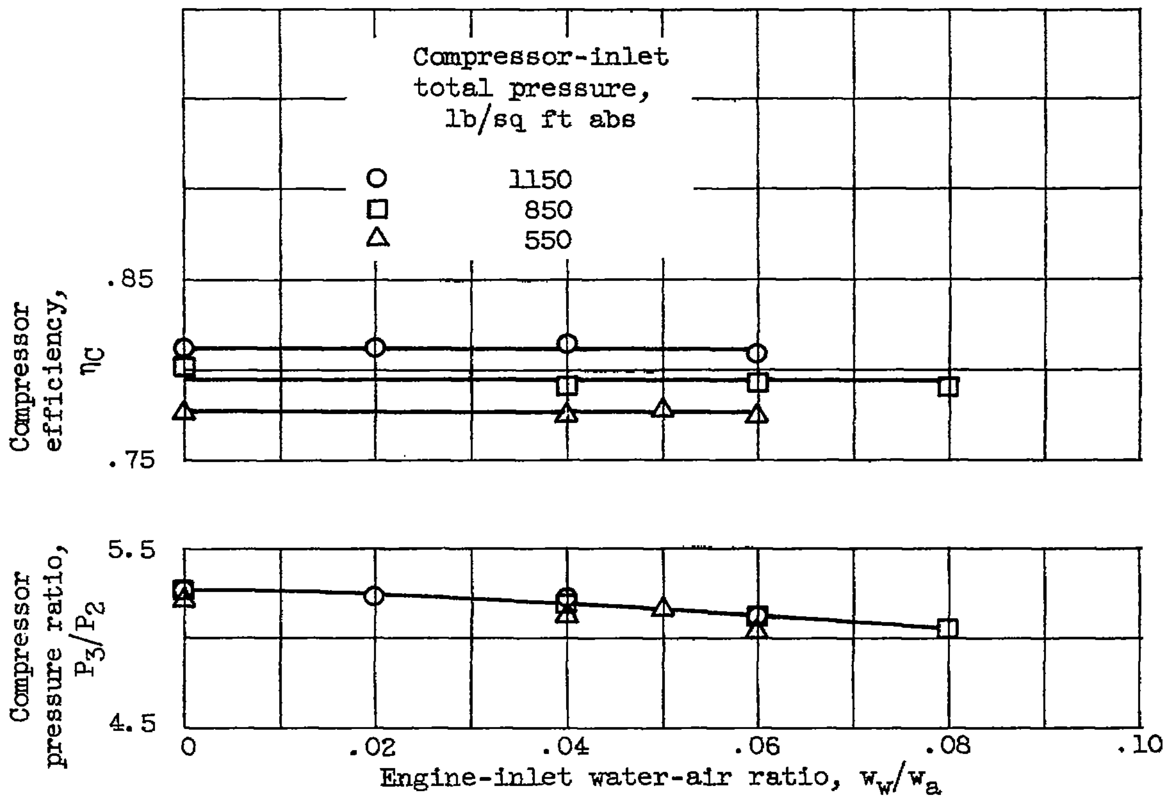

(a) Compressor efficiency and total-pressure ratio.

Figure 6. - Effects of engine-inlet water injection on compressor, combustor, and turbine performance.

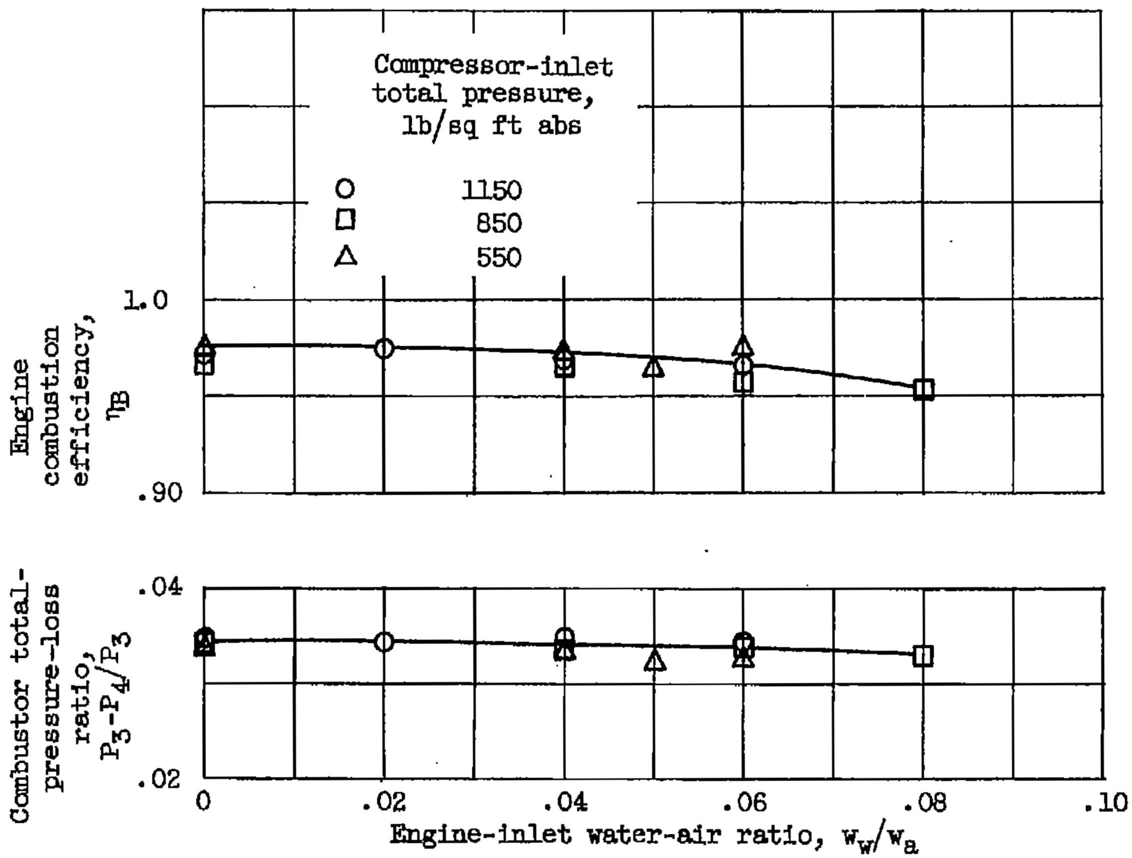

(b) Combustor efficiency and total-pressure-loss ratio.

Figure 6. - Continued. Effects of engine-inlet water injection on compressor, combustor, and turbine performance.

4810

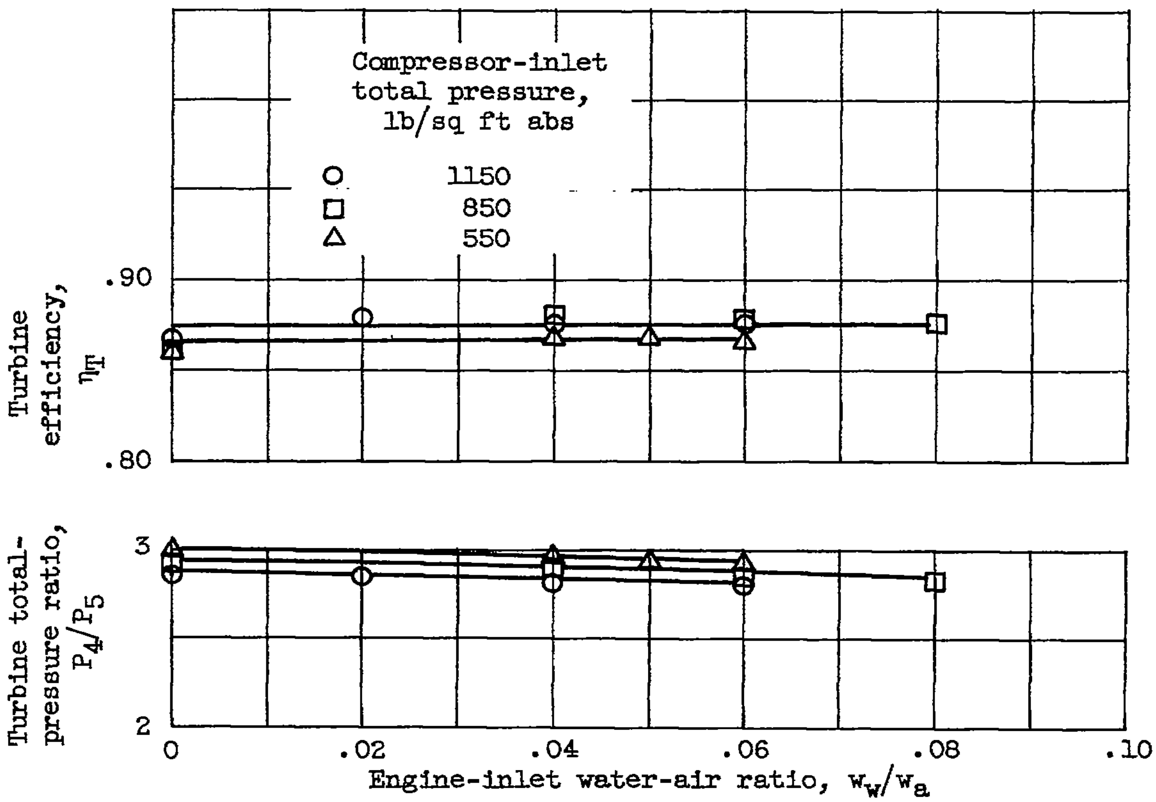

(c) Turbine efficiency and total-pressure ratio.

Figure 6. - Concluded. Effects of engine-inlet water injection on compressor, combustor, and turbine performance.

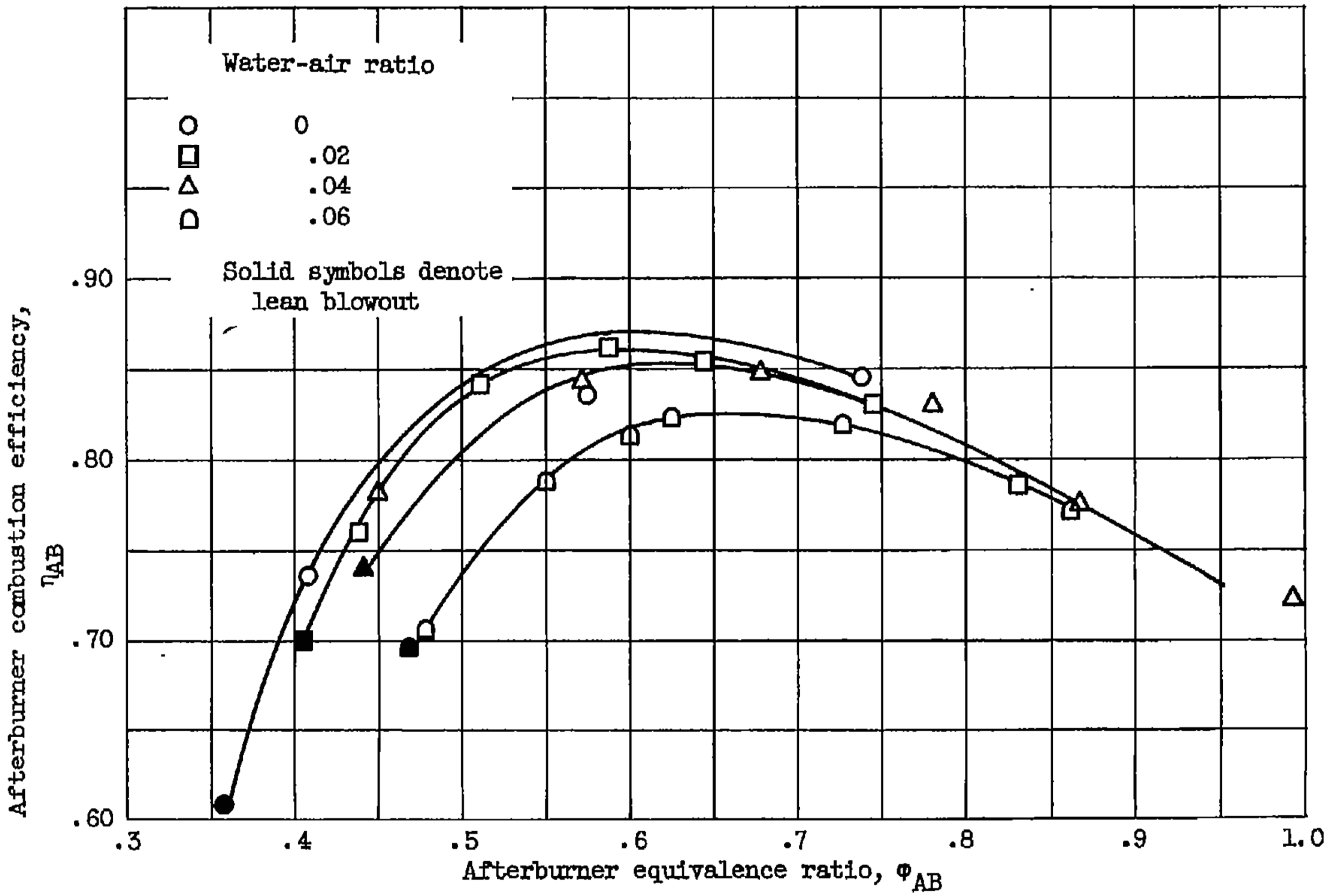

(a) Afterburner-inlet total pressure, 2000 pounds per square foot absolute.

Figure 7. - Effect of engine-inlet water injection on afterburner combustion efficiency.

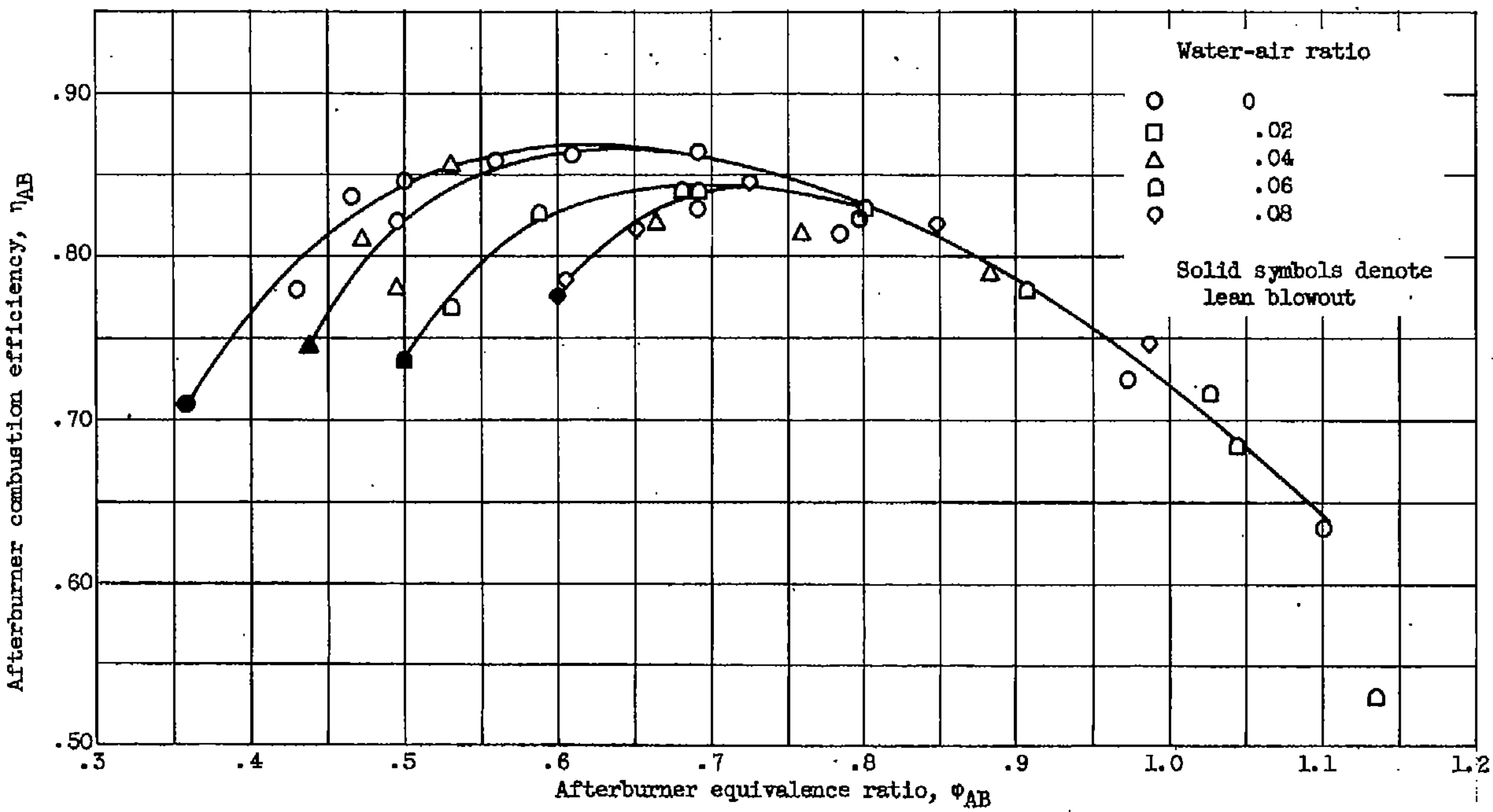

(b) Afterburner-inlet total pressure, 1500 pounds per square foot absolute.

Figure 7. - Continued. Effect of engine-inlet water injection on afterburner combustion efficiency.

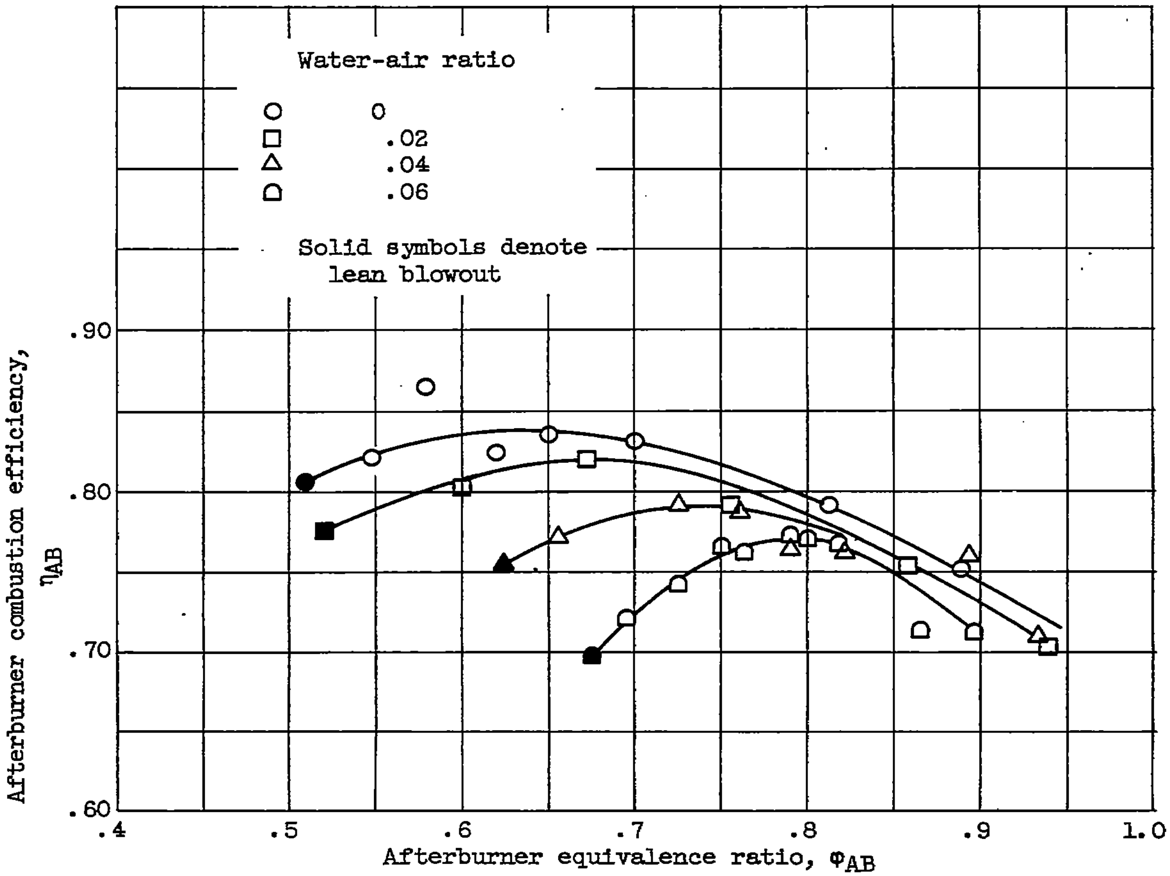

(c) Afterburner-inlet total pressure, 1000 pounds per square foot absolute.

Figure 7. - Concluded. Effect of engine-inlet water injection on afterburner combustion efficiency.

4810

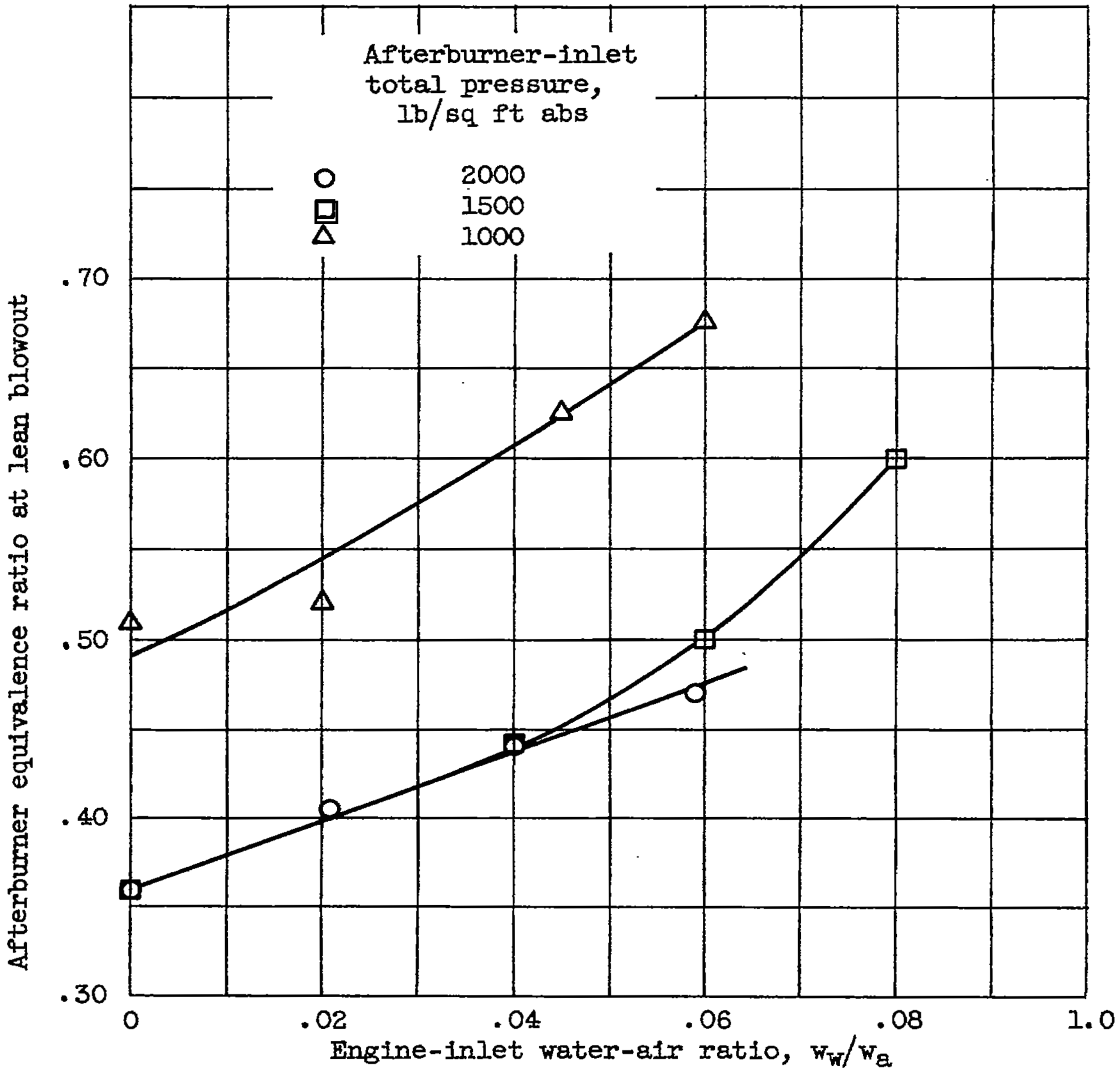

Figure 8. - Effect of afterburner-inlet total pressure and engine-inlet water-air ratio on afterburner lean blowout.

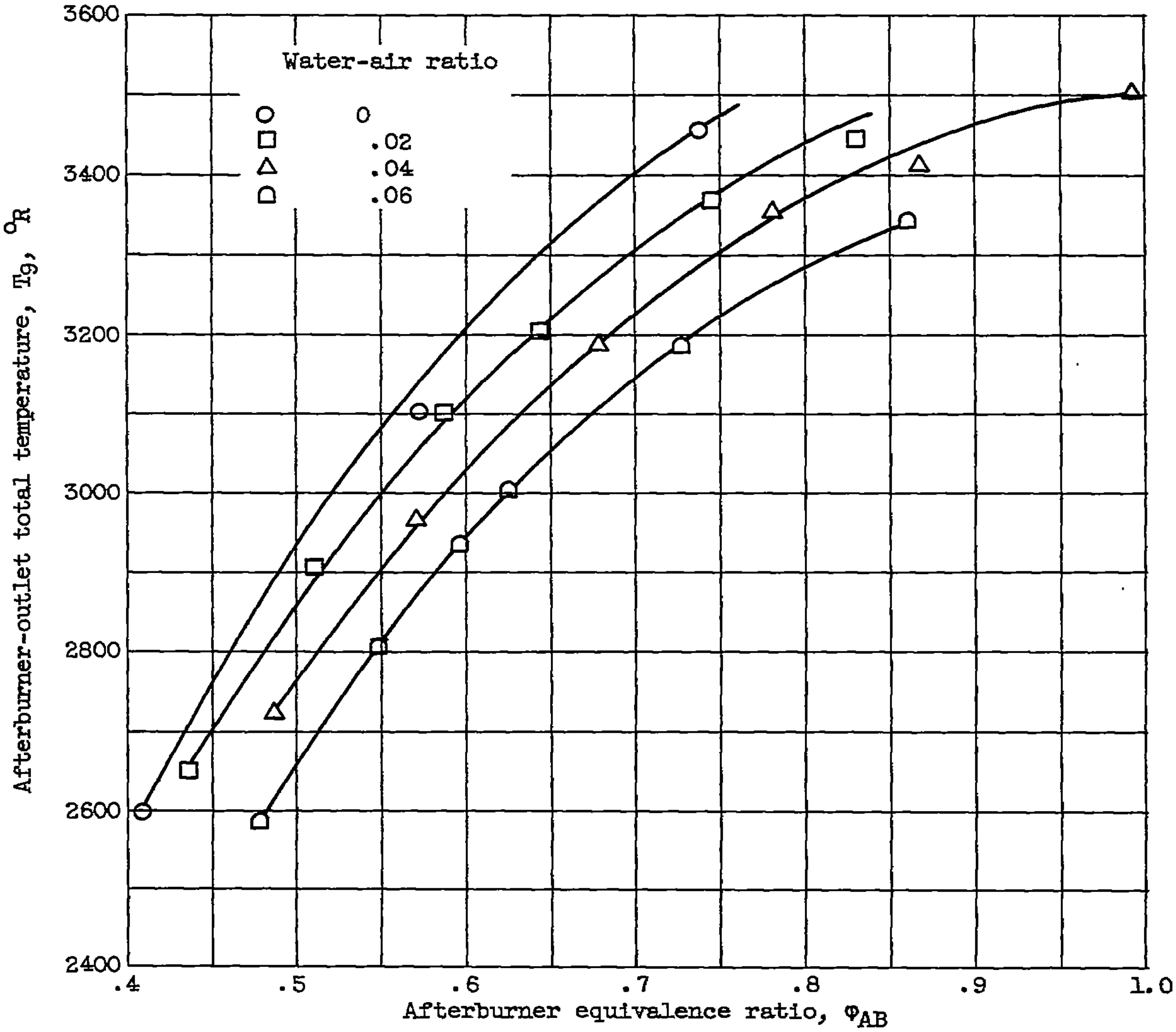

(a) Afterburner-inlet total pressure, 2000 pounds per square foot absolute.

Figure 9. - Effect of engine-inlet water injection on afterburner-outlet total temperature.

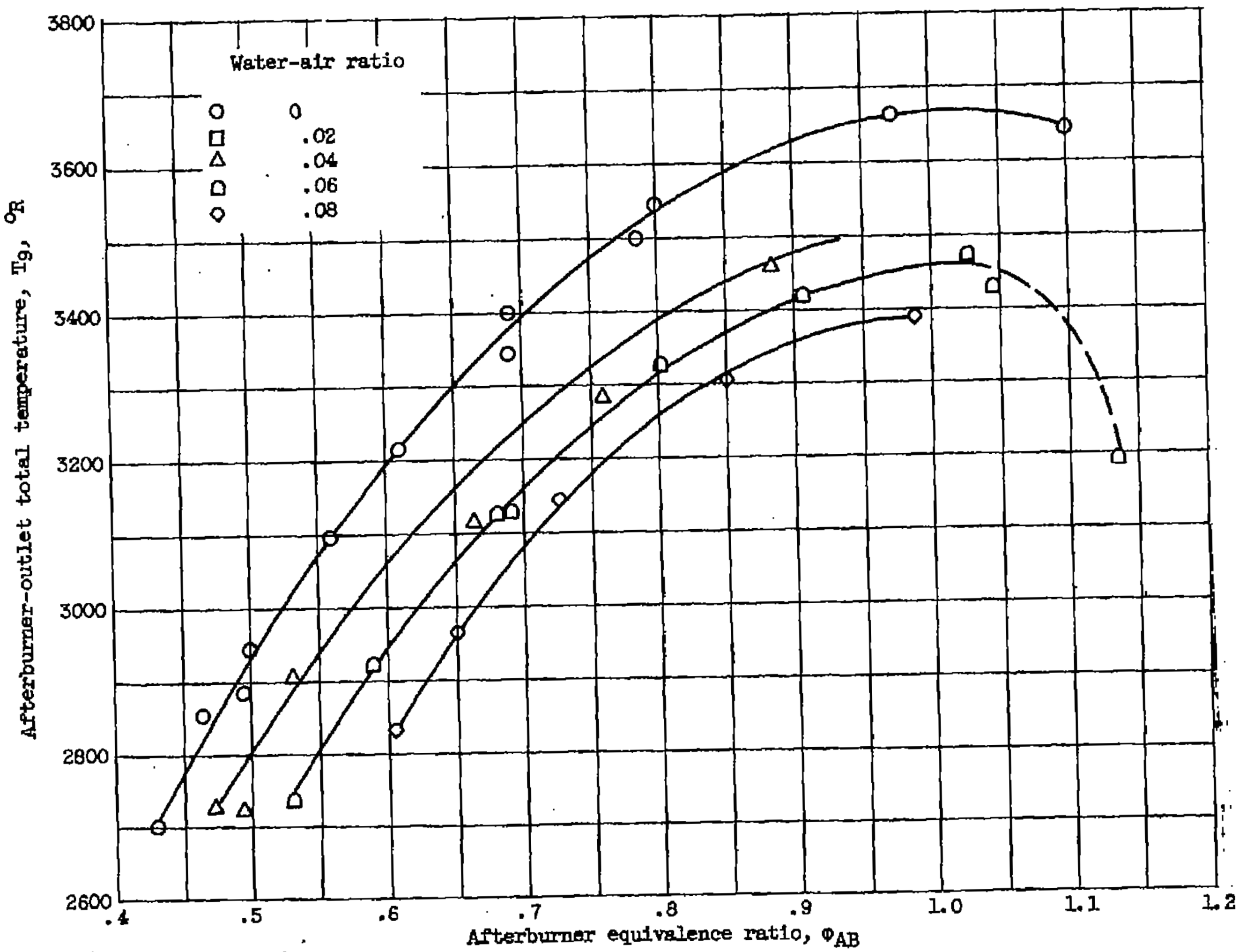

(b) Afterburner-inlet total pressure, 1500 pounds per square foot absolute.

Figure 9. - Continued. Effect of engine-inlet water injection on afterburner-outlet total temperature.

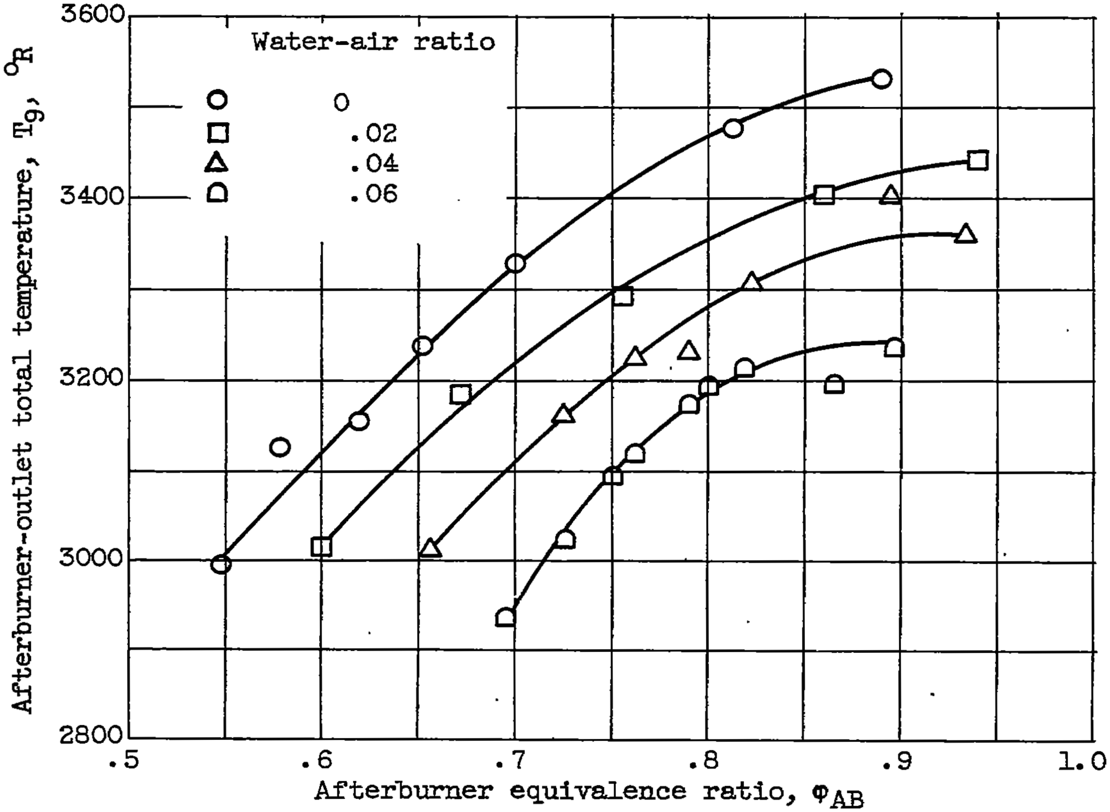

(c) Afterburner-inlet total pressure, 1000 pounds per square foot absolute.

Figure 9. - Concluded. Effect of engine-inlet water injection on afterburner-outlet total temperature.

4810

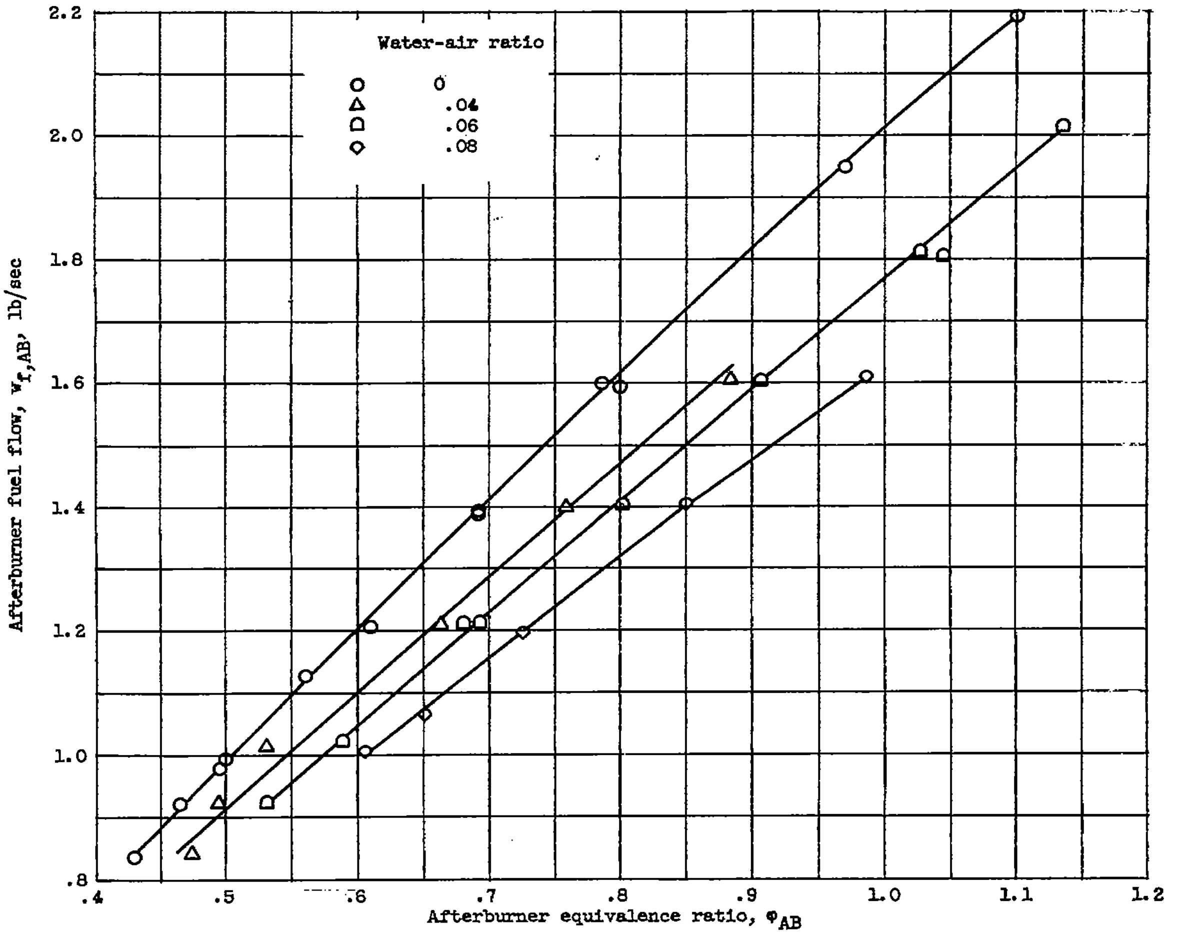

Figure 10. - Effect of engine-inlet water injection on afterburner fuel flow at an afterburner-inlet total pressure of 1500 pounds per square foot absolute.

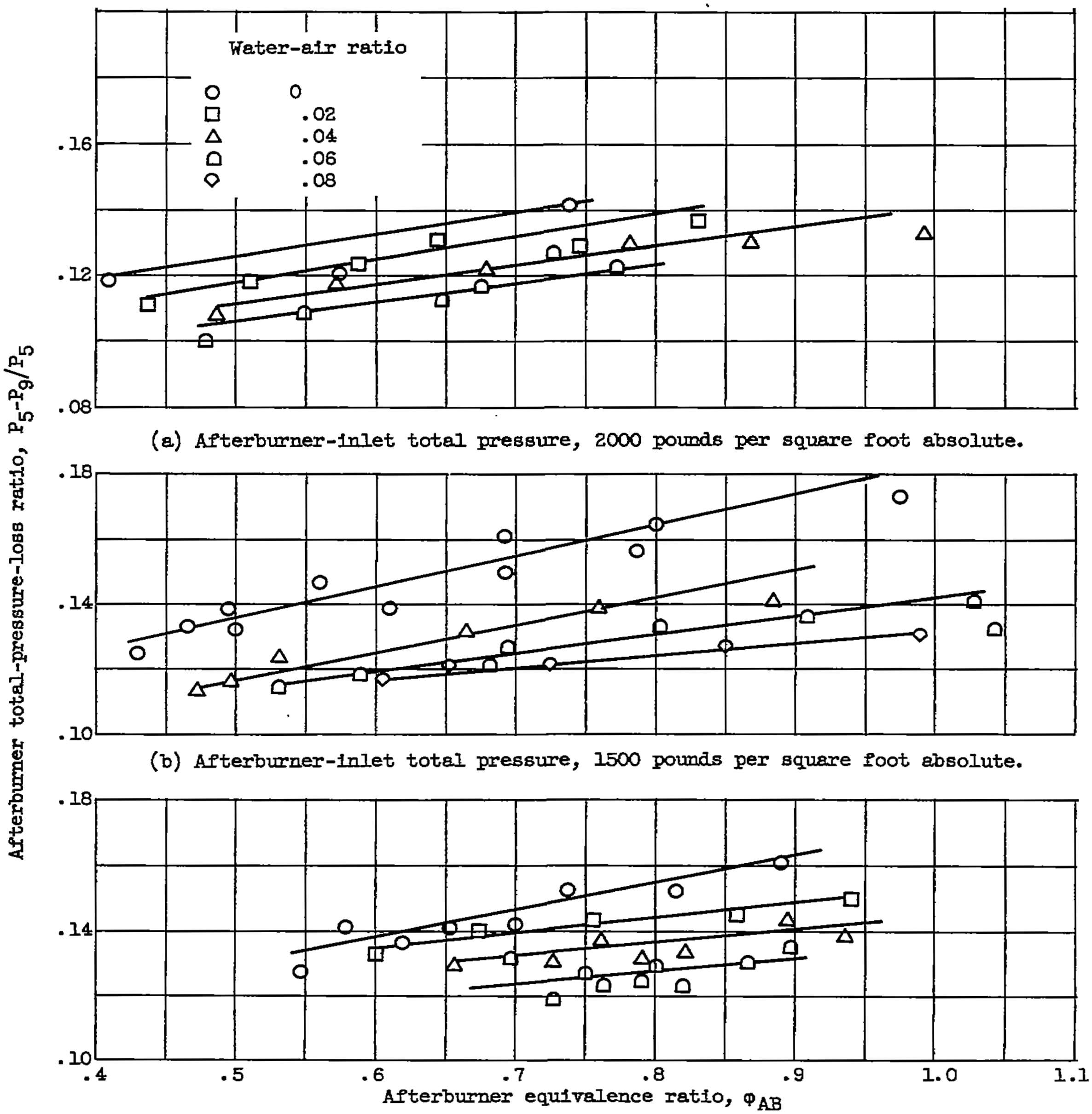

(a) Afterburner-inlet total pressure, 2000 pounds per square foot absolute.

(b) Afterburner-inlet total pressure, 1500 pounds per square foot absolute.

(c) Afterburner-inlet total pressure, 1000 pounds per square foot absolute.

Figure 11. - Effect of engine-inlet water injection on the afterburner total-pressure-loss ratio.

[redacted]

4810

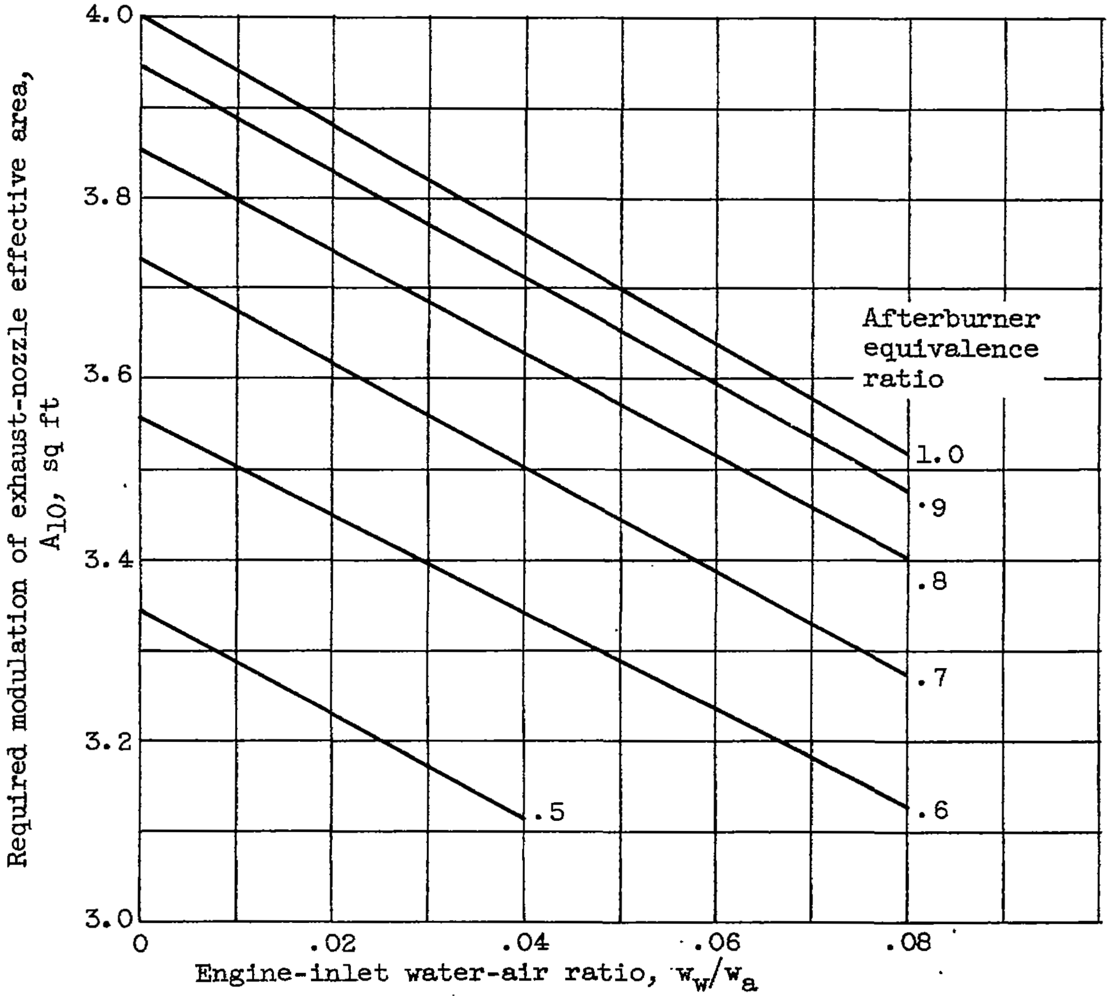

Figure 12. - Effect of engine-inlet water injection on the effective exhaust-nozzle area required for constant turbine-outlet gas temperature operation.

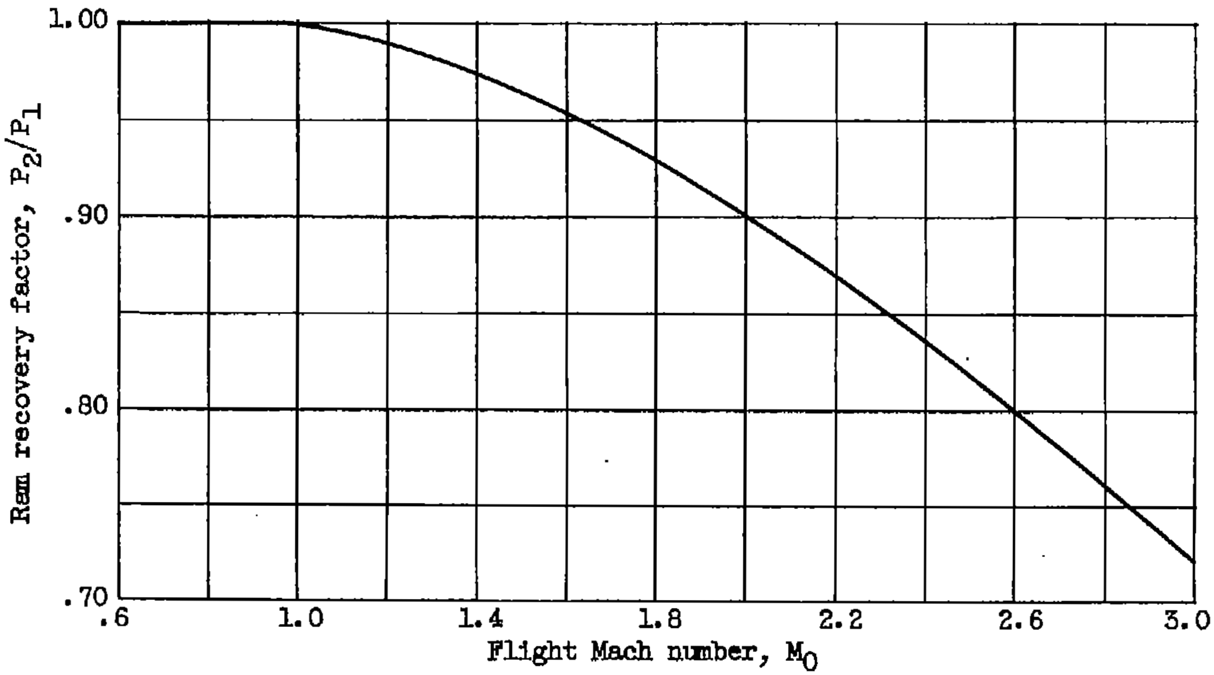

Figure 13. - Aircraft Industries Association standard inlet ram recovery.

4810

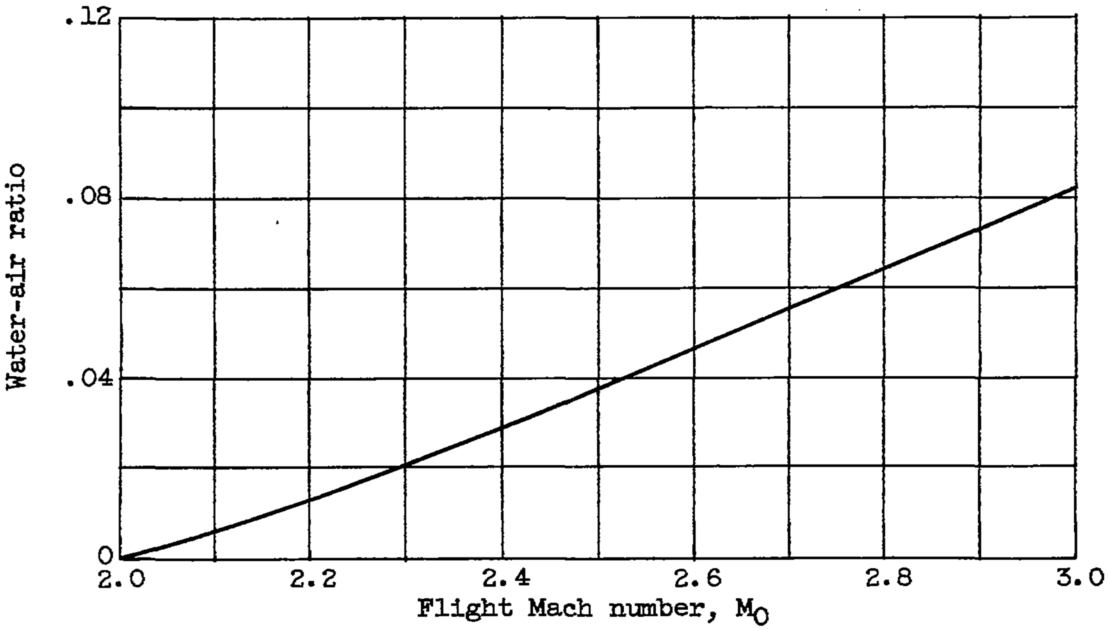

Figure 14. - Engine-inlet water-air ratio required to maintain constant compressor-inlet total temperature with increasing Mach number.

4810

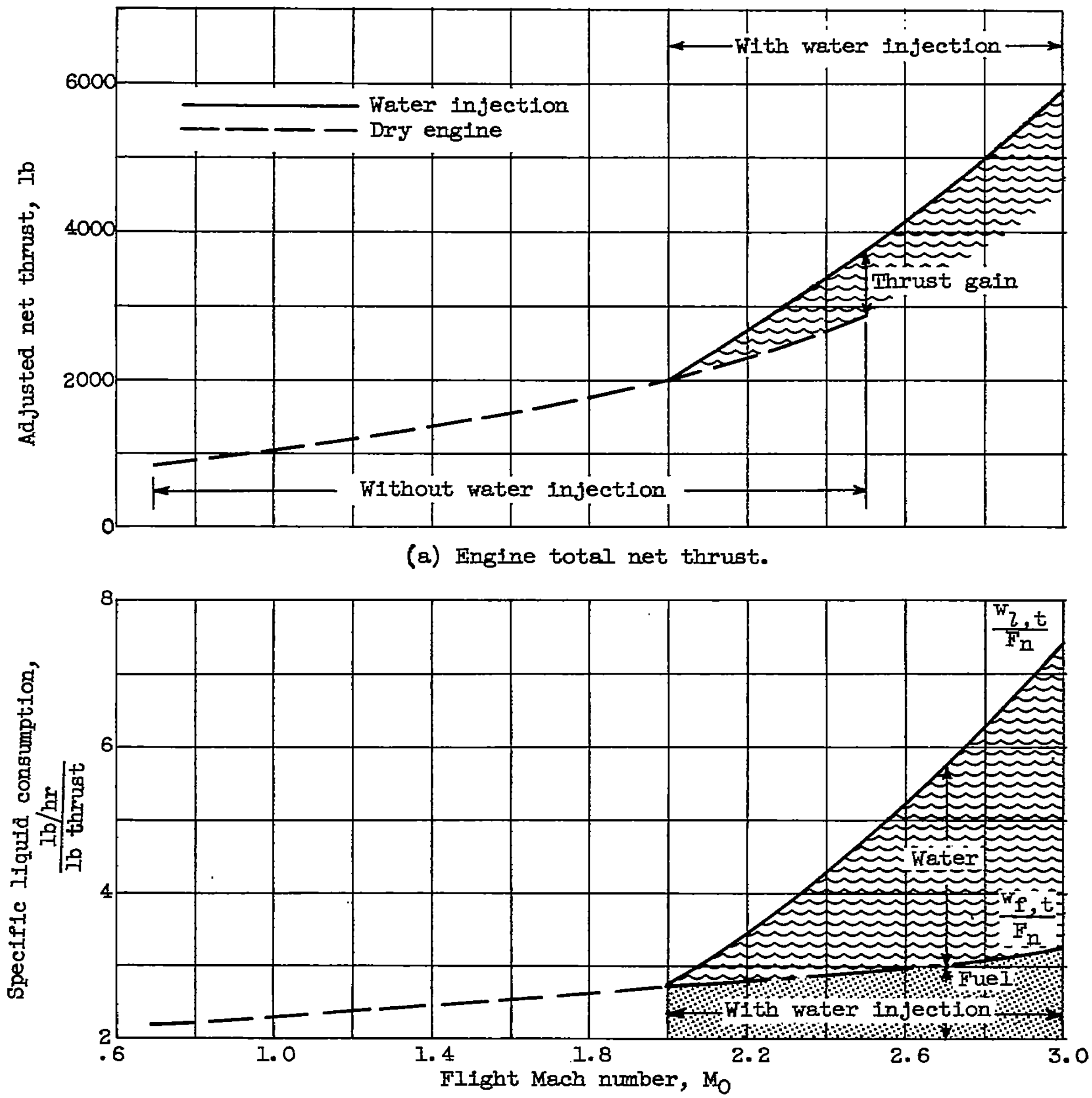

(a) Engine total net thrust.

(b) Net thrust specific liquid consumption.

Figure 15. - Over-all engine and afterburner performance at constant altitude and increasing flight Mach number with water injection.

[redacted]

DO NOT REMOVE SLIP FROM MATERIAL

Delete your name from this slip when returning material to the library.

NAME	DATE	MS
~~C. Domack~~	~~10/9/92~~	~~472~~

NASA Langley (Rev. Dec. 1991) RIAD N-75

UNCLASSIFIED

[redacted]

~~CONFIDENTIAL~~